

## 16-Bit, 15 MSPS, $\mu$ Module Data Acquisition Solution

### FEATURES

- ▶ Integrated fully differential ADC driver with signal scaling
  - ▶ Wide input common-mode voltage range
  - ▶ High common-mode rejection
- ▶ Single-ended to differential conversion
- ▶ Pin selectable input range with overrange
  - ▶ Input ranges with 4.096 V REFBUF:  $\pm 10$  V,  $\pm 5$  V,  $\pm 4.096$  V,  $\pm 2.5$  V, and  $\pm 1.5$  V
- ▶ Gain/attenuation options: 0.37, 0.73, 0.87, 1.38, and 2.25
  - ▶ Critical passive components
  - ▶ 0.005% precision matched resistor array for FDA
- ▶ **9 mm  $\times$  9 mm, 0.8 mm pitch, 100-ball CSP\_BGA package**
  - ▶ 2.5 $\times$  footprint reduction vs. discrete solution
- ▶ Low power, dynamic power scaling, power-down mode
  - ▶ 143 mW typical at 15 MSPS
- ▶ Throughput: 15 MSPS, no pipeline delay
- ▶ INL error:  $\pm 9.2$  ppm typical,  $\pm 18.3$  ppm maximum
  - ▶ (Gain = 0.73, gain = 0.87, gain = 1.38, gain = 2.25)
- ▶ SINAD: 90 dB typical at 1 kHz (gain = 0.37 and gain = 0.73)
- ▶ THD:  $-121$  dB at 1 kHz,  $-112$  dB at 100 kHz (gain = 0.73)
- ▶ Gain error:  $\pm 0.005\%$ FS typical
- ▶ Gain error drift:  $\pm 0.11$  ppm/ $^{\circ}$ C typical
- ▶ On-board reference buffer with VCMO generation
- ▶ Serial LVDS interface
- ▶ Wide operating temperature range:  $-40^{\circ}$ C to  $+85^{\circ}$ C

- ▶ Mass spectrometry
- ▶ Traveling wave fault location
- ▶ Medical imaging and instruments

### GENERAL DESCRIPTION

The ADAQ23876 is a precision, high speed,  $\mu$ Module<sup>®</sup> data acquisition solution that reduces the development cycle of precision measurement systems by transferring the design burden of component selection, optimization, and layout from the designer to the device.

Using system-in-package (SIP) technology, the ADAQ23876 reduces end system component count by combining multiple common signal processing and conditioning blocks in a single device, including a low noise, fully differential ADC driver amplifier (FDA), a stable reference buffer, and a high speed, 16-bit, 15 MSPS successive approximation register (SAR) ADC.

The ADAQ23876 also incorporates the critical passive components with superior matching and drift characteristics using Analog Devices, Inc., iPassive<sup>®</sup> technology to minimize temperature dependent error sources and to offer optimized performance. The fast settling of the ADC driver stage and no latency of the SAR ADC provide a unique solution for high channel count, multiplexed signal chain architectures and control loop applications.

The small footprint, **9 mm  $\times$  9 mm, 0.8 mm pitch, 100-ball CSP\_BGA package** enables smaller form factor instruments without sacrificing performance. The system integration solves many design challenges while the device still provides the flexibility of a configurable ADC driver feedback loop to allow gain or attenuation adjustments, as well as fully differential or single-ended to differential input. A single 5 V supply operation is possible while achieving optimum performance from the device.

The ADAQ23876 features a serial low voltage differential signaling (LVDS) digital interface with one-lane or two-lane output modes, allowing the user to optimize the interface data rate for each application. The specified operation of the ADAQ23876 is from  $-40^{\circ}$ C to  $+85^{\circ}$ C.

### APPLICATIONS

- ▶ Automatic test equipment
- ▶ Data acquisition
- ▶ Hardware in the Loop (HiL)
- ▶ Power analyzers
- ▶ Nondestructive test (acoustic emissions)

### FUNCTIONAL BLOCK DIAGRAM

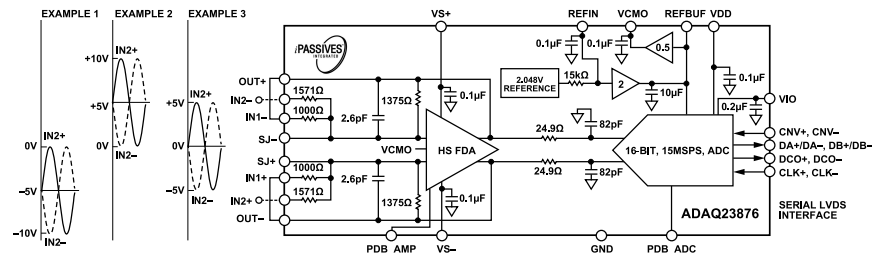


Figure 1. ADAQ23876 Configured for Gain = 0.37,  $\pm 10$  V Differential Input Range

**TABLE OF CONTENTS**

Features.....	1	Transfer Function .....	25
Applications.....	1	Applications Information.....	26
General Description.....	1	Typical Application Diagrams .....	26
Functional Block Diagram.....	1	Voltage Reference Input.....	30
Specifications.....	3	Common-Mode Output.....	30
Timing Specifications.....	7	Power Supply.....	30
Absolute Maximum Ratings.....	9	Digital Interface.....	32
Thermal Resistance.....	9	One-Lane Output Mode .....	32
Electrostatic Discharge (ESD) Ratings.....	9	Two-Lane Output Mode .....	32
ESD Caution.....	9	Output Test Patterns .....	35
Pin Configuration and Function Descriptions.....	10	Board Layout .....	36
Typical Performance Characteristics.....	12	Mechanical Stress Shift .....	36
Terminology.....	23	Outline Dimensions .....	37
Theory of Operation.....	25	Ordering Guide.....	37
Circuit Information .....	25	Evaluation Boards.....	37

**REVISION HISTORY****2/2026—Rev. A to Rev. B**

Changes to Features Section.....	1
Changes to Table 1.....	3
Changes to Figure 3.....	8
Changes to Figure 16.....	13
Changes to Figure 21 Caption to Figure 23 Caption.....	14
Changes to Figure 24 Caption and Figure 25 Caption.....	15
Changes to Figure 60 to Figure 64.....	21
Change to Offset Error Drift Section.....	23
Change to Gain Error Drift Section.....	23
Change to Table 7.....	25
Changes to Figure 86 and Figure 87.....	33

**2/2023—Rev. 0 to Rev. A**

Changes to Transition Noise Parameter; Dynamic Range Parameter; Total RMS Noise, Referred to Output (RTO) Parameter; and Input Voltage Noise Parameter, Table 1.....	3
Change to Figure 81.....	30
Change to Figure 82.....	30

**1/2022—Revision 0: Initial Version**

## SPECIFICATIONS

VDD = 5 V ± 5%, VS+ = 5 V ± 5%, VS- = -1 V ± 5%, VS- = 0 V (95% of VIN), VIO = 2.375 V to 2.625 V, REFBUF = 4.096 V, sampling frequency (fS) = 15 MSPS, gain = 0.37, 0.73, 0.87, 1.38, and 2.25, and all specifications TMIN to TMAX, unless otherwise noted. For all gain values, limit the differential input range, VIN, to 95% to allow enough footroom for the ADC driver with VS- = 0 V to achieve the specified performance.

Table 1.

Parameter	Test Conditions/Comments	Min	Typ	Max	Unit <sup>1</sup>
RESOLUTION		16			Bits
ANALOG INPUT IMPEDANCE, ZIN	IN1+, IN1-, IN2+, IN2-, SJ+, and SJ- single-ended to differential configuration Gain = 0.37 (resistor gain (RG) = 1571 Ω, resistor feedback (RF) = 1375 Ω    1000 Ω) Gain = 0.73 (RG = 1000 Ω, RF = 1571 Ω <sup>2</sup>    1375 Ω) Gain = 0.87 (RG = 1571 Ω, RF = 1375 Ω) Gain = 1.38 (RG = 1000 Ω, RF = 1375 Ω) Gain = 2.25 (RG = 1571 Ω    1000 Ω, RF = 1375 Ω) Fully differential configuration Gain = 0.37 (RG = 1571 Ω, RF = 1375 Ω    1000 Ω) Gain = 0.73 (RG = 1000 Ω, RF = 1571 Ω    1375 Ω) Gain = 0.87 (RG = 1571 Ω, RF = 1375 Ω) Gain = 1.38 (RG = 1000 Ω, RF = 1375 Ω) Gain = 2.25 (RG = 1571 Ω    1000 Ω, RF = 1375 Ω)		1816 1268 2050 1407 935 3143 2000 3143 2000 1222		Ω Ω Ω Ω Ω Ω Ω Ω Ω Ω
Input Capacitance	IN1+, IN1-		3.3		pF
Differential Input Voltage Range, VIN <sup>3,4</sup>	Gain = 0.37, VIN = 22.2 V p-p Gain = 0.73, VIN = 11.2 V p-p Gain = 0.87, VIN = 9.4 V p-p Gain = 1.38, VIN = 5.9 V p-p Gain = 2.25, VIN = 3.6 V p-p	-11.1 -5.6 -4.7 -2.9 -1.8		+11.1 +5.6 +4.7 +2.9 +1.8	V V V V V
THROUGHPUT					
Complete Cycle		66.6			ns
Conversion Time		54	58	63	ns
Acquisition Phase <sup>5</sup>			Time between conversions (tCYC) - 39		ns
Throughput Rate <sup>6</sup>		0.02		15	MSPS
Transient Response <sup>7</sup>	Full-scale step		52		ns
DC ACCURACY	Single-ended and differential configuration				
No Missing Codes		16			Bits
Integral Nonlinearity (INL) Error	Gain = 0.37 single-ended	-2.0 -30.5	-1.6 -24.4	+0.4 +6.1	LSB ppm
	Gain = 0.37 differential	-1.0 -15.3	±0.4 ±6.1	+1.0 +15.3	LSB ppm
	Gain = 0.73, gain = 0.87, gain = 1.38, and gain = 2.25	-1.2 -18.3	±0.6 ±9.2	+1.2 +18.3	LSB ppm
Differential Nonlinearity (DNL) Error	All gains	-0.9 -13.7	±0.4 ±6.1	+0.9 +13.7	LSB ppm
Transition Noise	Gain = 0.37 and gain = 0.73 Gain = 0.87, gain = 1.38, and gain = 2.25		0.65 0.69		LSBRMS LSBRMS
Gain Error	All gains	-0.025	±0.005	+0.025	%FS
Gain Error Drift		-0.46	±0.11	+0.46	ppm/°C

## SPECIFICATIONS

Table 1. (Continued)

Parameter	Test Conditions/Comments	Min	Typ	Max	Unit <sup>1</sup>
Offset Error		-2.5	+0.3	+2.5	mV
Offset Error Drift		-9	±2.2	+9	ppm/°C
Common-Mode Rejection Ratio (CMRR), Input Referred	$\Delta V_{ICM}/\Delta V_{OSDIFF}$  All gains		98		dB
Power Supply Rejection Ratio (PSRR) Positive	VDD = 4.75 V to 5.25 V All gains		103		dB
Negative	VS+ = +5 V, VS- = -0.75 V to -1.25 V All gains		103		dB
1/f Noise <sup>8</sup>	Bandwidth = 0.1 Hz to 10 Hz		9		μV p-p
Input Current Noise	f = 100 kHz		1		pA/√Hz
AC ACCURACY <sup>9</sup>	Single-ended and differential configuration				
Dynamic Range	Input frequency (f <sub>IN</sub> ) = 1 kHz, -60 dB input Gain = 0.37 and gain = 0.73	86.5	91		dB
	Gain = 0.87, gain = 1.38, and gain = 2.25		90.5		dB
Total RMS Noise, Referred to Output (RTO)	Gain = 0.37 and gain = 0.73		81.6		μV <sub>RMS</sub>
	Gain = 0.87, gain = 1.38, and gain = 2.25		86.47		μV <sub>RMS</sub>
Input Voltage Noise Density	Gain = 0.37		80.9		nV/√Hz
	Gain = 0.73		40.7		nV/√Hz
	Gain = 0.87		36.1		nV/√Hz
	Gain = 1.38		23		nV/√Hz
	Gain = 2.25		14		nV/√Hz
Signal-to-Noise Ratio (SNR)	f <sub>IN</sub> = 1 kHz, -1 dBFS Gain = 0.37 and gain = 0.73	85.5	90.7		dB
	Gain = 0.87, gain = 1.38, and gain = 2.25		89.8		dB
	f <sub>IN</sub> = 100 kHz Gain = 0.37 and gain = 0.73		90		dB
	Gain = 0.87, gain = 1.38, and gain = 2.25		89		dB
	f <sub>IN</sub> = 1 MHz Gain = 0.73		83.1		dB
	Gain = 0.87 and gain = 1.38		82		dB
	Gain = 2.25		80.7		dB
Signal-to-Noise-and-Distortion (SINAD)	f <sub>IN</sub> = 1 kHz Gain = 0.37 and gain = 0.73	85.4	90		dB
	Gain = 0.87, gain = 1.38, and gain = 2.25		88.8		dB
	f <sub>IN</sub> = 100 kHz Gain = 0.37 and gain = 0.73		88.5		dB
	Gain = 0.87, gain = 1.38, and gain = 2.25		88		dB
	f <sub>IN</sub> = 1 MHz Gain = 0.73		72.7		dB
	Gain = 0.87		70.1		dB
	Gain = 1.38		68.8		dB
	Gain = 2.25		66.6		dB
Total Harmonic Distortion (THD)	f <sub>IN</sub> = 1 kHz Gain = 0.37		-106.9		dB
	Gain = 0.73		-121		dB
	Gain = 0.87		-118		dB
	Gain = 1.38 and gain = 2.25		-114.5		dB

## SPECIFICATIONS

Table 1. (Continued)

Parameter	Test Conditions/Comments	Min	Typ	Max	Unit <sup>1</sup>
Spurious-Free Dynamic Range (SFDR)	$f_{IN} = 100$ kHz				
	Gain = 0.37 and gain = 2.25		-109		dB
	Gain = 0.73, gain = 0.87, and gain = 1.38		-112		dB
	$f_{IN} = 1$ MHz				
	Gain = 0.73		-73.3		dB
	Gain = 0.87		-70.5		dB
	Gain = 1.38		-69		dB
	Gain = 2.25		-66.8		dB
	$f_{IN} = 1$ kHz				
	Gain = 0.37		106.4		dB
	Gain = 0.73 and gain = 0.87		123		dB
	Gain = 1.38		117.1		dB
	Gain = 2.25		115.5		dB
	-3 dB Input Bandwidth, RC Filter	$f_{IN} = 100$ kHz			
Gain = 0.37			100		dB
Gain = 0.73, gain = 0.87, gain = 1.38, and gain = 2.25			104		dB
$f_{IN} = 1$ MHz					
Gain = 0.73			74.8		dB
Gain = 0.87			71.8		dB
Gain = 1.38			70.5		dB
Gain = 2.25			68.1		dB
Output voltage ( $V_{OUT}$ ) differential ( $V_{OUTDIFF}$ ) = 2 V p-p					
Gain = 0.37			54.4		MHz
Gain = 0.73			45.7		MHz
Gain = 0.87			30.5		MHz
Gain = 1.38			27.8		MHz
Gain = 2.25			26.6		MHz
Aperture Delay <sup>10</sup>			0		ns
Aperture Jitter <sup>11</sup>			0.25		ps <sub>RMS</sub>
REFERENCE					
REFIN, Internal Reference Output Voltage	Output current ( $I_{OUT}$ ) = 0 $\mu$ A	2.028	2.048	2.068	V
Temperature Coefficient			$\pm 5$	$\pm 20$	ppm/ $^{\circ}$ C
Output Impedance			15		k $\Omega$
Line Regulation	VDD = 4.75 V to 5.25 V		0.3		mV/V
Input Voltage Range	REFIN overdriven	2.028	2.048	2.068	V
Reference Buffer Output Voltage, REFBUF	REFIN = 2.048 V	4.056	4.096	4.136	V
Input Voltage Range	REFBUF overdriven <sup>11</sup>	4.056	4.096	4.136	V
Load Current	REFBUF = 4.096 V (REFBUF overdriven)		1.75	1.95	mA
	REFBUF = 4.096 V (REFBUF overdriven)		0.5		mA
VCMO <sup>12</sup>					
Common-Mode Output Voltage	REFBUF = 4.096 V, $I_{OUT} = 0$ $\mu$ A	2.028	2.048	2.028	V
Output Impedance	-1 mA < $I_{OUT}$ < +1 mA		15		$\Omega$
DIGITAL INPUTS					
Logic Levels					
Input Low Voltage, $V_{IL}$	VIO = 2.5 V			0.6	V
Input High Voltage, $V_{IH}$	VIO = 2.5 V	1.7			V
Digital Input Current	$V_{IN} = 0$ V to 2.5 V	-10		+10	$\mu$ A
Input Pin Capacitance			3		pF

## SPECIFICATIONS

Table 1. (Continued)

Parameter	Test Conditions/Comments	Min	Typ	Max	Unit <sup>1</sup>
CNV+/CNV– and CLK+/CLK– (LVDS Clock Input) Differential Input Voltage, $V_{ID}$ Common-Mode Input Voltage, $V_{ICM}$		175	350	650	mV
DCO+/DCO–, DA+/DA–, DB+/DB– (LVDS Outputs)		0.8	1.25	1.7	V
Differential Output Voltage, $V_{OD}$	100 $\Omega$ differential load	247	350	454	mV
Common-Mode Output Voltage, $V_{OS}$	100 $\Omega$ differential load	1.125	1.25	1.375	V
POWER-DOWN MODE					
ADC Driver (PDB_AMP)/ADC (PDB_ADC)					
Low	Power-down mode		<1		V
High	Enabled, normal operation		>1.7		V
POWER REQUIREMENTS					
VDD		4.75	5	5.25	V
VS+		3	5	VS– + 10	V
VS–		VS+ – 10	0	+0.1	V
VIO		2.375	2.5	2.625	V
Total Standby Current <sup>13, 14</sup>	Static, all devices enabled		45	52	mA
	Static, all devices disabled		0.1	0.4	$\mu$ A
ADAQ23876 Current Draw					
VDD			4.6	5.5	mA
VS+/VS–			4	5.5	mA
VIO			40	42	mA
ADAQ23876 Power Dissipation					
VDD	VDD = 5 V, VS+ = 5 V, VS– = 0 V		19	26.25	mW
VS+/VS–	Gain = 0.37		24	28.875	mW
VIO	One-lane mode <sup>15</sup>		100	110.25	mW
Total			143	165.375	mW
TEMPERATURE RANGE					
Specified Performance	$T_{MIN}$ to $T_{MAX}$	–40		+85	$^{\circ}$ C

<sup>1</sup> The LSB unit means least significant bit. The weight of the LSB, referred to input, changes depending on the input voltage range.

<sup>2</sup> For accurate resistor iPassive value  $IN2_{\pm}$ , gain resistor ( $R_G$ ) = 1.5714286 k $\Omega$ .

<sup>3</sup> The differential input ranges,  $V_{IN}$ , must be within the allowed input common-mode range as per Figure 60 to Figure 64.  $V_{IN}$  is dependent on the VS+/VS– supply rails used.

<sup>4</sup> For exact values of differential input range, use the equation  $V_{IN} = REFBUF/Gain$ , where  $Gain = R_F/R_G$ .

<sup>5</sup> The acquisition phase is the time available for the input sampling capacitors to acquire a new input with the ADAQ23876 running at a throughput rate of 15 MSPS.

<sup>6</sup>  $f_S = 15$  MHz, and the REFBUF current ( $I_{REFBUF}$ ) varies linearly with the throughput rate.

<sup>7</sup> Transient response is the time required for the ADAQ23876 to acquire a full-scale input step to within  $\pm 1$  LSB accuracy. Guaranteed by design, not subject to test.

<sup>8</sup> See the 1/f noise plot in Figure 65.

<sup>9</sup> All ac specifications expressed in decibels are referenced to the full-scale input range (FSR) and are tested with an input signal at 1 dB below full scale, unless otherwise specified.

<sup>10</sup> Guaranteed by design, not subject to test.

<sup>11</sup> When REFBUF is overdriven, turn off the internal reference buffer by setting  $REFIN = 0$  V. Refer to the Voltage Reference Input section for more information.

<sup>12</sup> The VCMO voltage can be used for other circuitry. However, drive the voltage with a buffer to ensure the VCMO voltage remains stable as per the specified range.

<sup>13</sup> With all digital inputs forced to VIO or GND, as required.

<sup>14</sup> During the acquisition phase.

<sup>15</sup> In two-lane mode, the VIO power dissipation is about 10 mW higher than one-lane mode.



SPECIFICATIONS

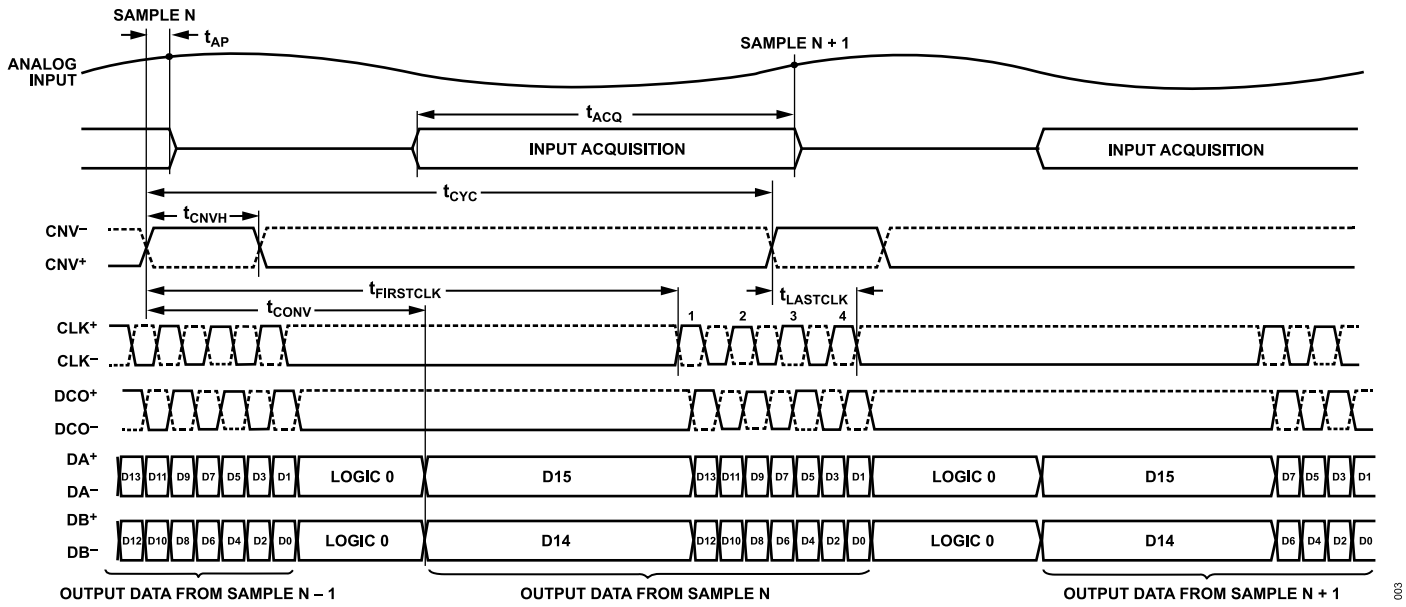


Figure 3. Two-Lane Output Mode Timing Diagram

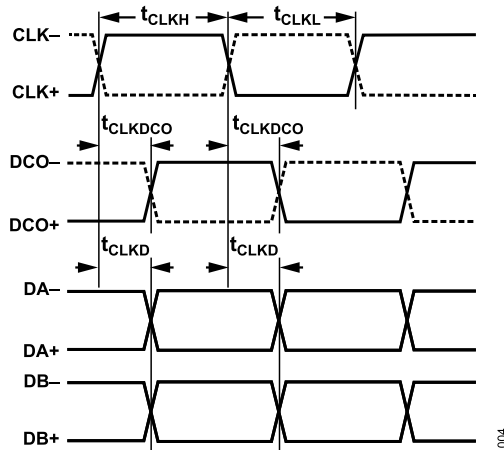


Figure 4. Data Output Timing Diagram

## ABSOLUTE MAXIMUM RATINGS

Table 3.

Parameter	Rating
Analog Inputs	
IN1+, IN1- to GND	-12 V to +12 V or 8 mA
IN2+, IN2- to GND	-12 V to +12 V or 12 mA
Supply Voltage	
VDD to GND	6 V
VIO to GND	2.8 V
VS+ to VS-	11 V
VS+ to GND	-0.3 V to +11 V
VS- to GND	-11 V to +0.3 V
REFBUF to GND	-0.3 V to VDD + 0.3 V
REFIN to GND	-0.3 V to +2.8 V
Digital Inputs to GND	-0.3 V to VIO + 0.3 V
Storage Temperature Range	-65°C to +150°C
Junction Temperature	150°C
Lead Temperature Soldering	260°C reflow as per JEDEC J-STD-020

Stresses at or above those listed under Absolute Maximum Ratings may cause permanent damage to the product. This is a stress rating only; functional operation of the product at these or any other conditions above those indicated in the operational section of this specification is not implied. Operation beyond the maximum operating conditions for extended periods may affect product reliability.

## THERMAL RESISTANCE

Thermal performance is directly linked to printed circuit board (PCB) design and operating environment. Careful attention to PCB thermal design is required.

Table 4. Thermal Resistance

Package Type <sup>1</sup>	$\theta_{JA}$	$\Psi_{JT}$	$\Psi_{JB}$	$\theta_{JC}$			Unit
				BOTTOM	$\theta_{JC\ TOP}$	$\theta_{JB}$	
BC-100-7	48.43	4.64	27.89	9.9	35.15	33.24	°C/W

<sup>1</sup> Test Condition 1: thermal impedance simulated values are based on use of a 2S2P with vias JEDEC PCB excluding the  $\theta_{JC\ TOP}$  which uses 1S0P JEDEC PCB.

## ELECTROSTATIC DISCHARGE (ESD) RATINGS

The following ESD information is provided for the handling of ESD sensitive devices in an ESD protected area only.

The human body model (HBM) is per ANSI/ESDA/JEDDEC JS-001.

The field induced charged device model (FICDM) per ANSI/ESDA/JEDEC JS-002.

## ESD Ratings for ADAQ23876

Table 5. ADAQ23876, 100-Ball CSP\_BGA

ESD Model	Withstand Threshold (V)
HBM	2250
FICDM	1000

## ESD CAUTION



**ESD (electrostatic discharge) sensitive device.** Charged devices and circuit boards can discharge without detection. Although this product features patented or proprietary protection circuitry, damage may occur on devices subjected to high energy ESD. Therefore, proper ESD precautions should be taken to avoid performance degradation or loss of functionality.

## PIN CONFIGURATION AND FUNCTION DESCRIPTIONS

	1	2	3	4	5	6	7	8	9	10
A	GND	IN1-	IN1+	IN2-	IN2+	SJ-	GND	VIO	GND	CNV+
B	PDB_AMP	IN1-	IN1+	IN2-	IN2+	SJ+	GND	TWOLANES	GND	CNV-
C	OUT+	VS+	OUT-	VS+	VS-	GND	GND	GND	GND	GND
D	OUT+	GND	OUT-	GND	GND	VCMO	GND	GND	GND	CLK+
E	GND	GND	GND	VS+	GND	GND	GND	GND	GND	CLK-
F	NC	NC	GND	GND	GND	GND	GND	GND	GND	GND
G	GND	GND	GND	GND	GND	GND	GND	GND	GND	DCO+
H	VS+	GND	GND	GND	GND	GND	GND	GND	GND	DCO-
J	VS-	GND	REFBUF	REFBUF	GND	GND	GND	GND	GND	DA+
K	GND	GND	REFIN	GND	PDB_ADC	VDD	TESTPAT	DB-	DB+	DA-

Figure 5. 100-Ball CSP\_BGA Pin Configuration, Top View

Table 6. Pin Function Descriptions

Pin No.	Mnemonic	Type <sup>1</sup>	Description
A1, A7, A9, B7, B9, C6, C7, C8, C9, C10, D2, D4, D5, D7, D8, D9, E1, E2, E3, E5, E6, E7, E8, E9, F3, F4, F5, F6, F7, F8, F9, F10, G1, G2, G3, G4, G5, G6, G7, G8, G9, H2, H3, H4, H5, H6, H7, H8, H9, J2, J5, J6, J7, J8, J9, K1, K2, K4	GND	P	Power Supply Ground.
A2, B2	IN1-	AI	Negative Input of the FDA Connected to 1000 $\Omega$ Resistor.
A3, B3	IN1+	AI	Positive Input of the FDA Connected to 1000 $\Omega$ Resistor.
A4, B4	IN2-	AI	Negative Input of the FDA Connected to 1571 $\Omega$ Resistor.
A5, B5	IN2+	AI	Positive Input of the FDA Connected to 1571 $\Omega$ Resistor.
A6	SJ-	AI	Negative Input of the FDA.
B6	SJ+	AI	Positive Input of the FDA.
A8	VIO	P	2.5 V Analog and Output Power Supply. The range of VIO is 2.375 V to 2.625 V. Bypass this pin to GND with an at least 2.2 $\mu$ F (0402, X5R) ceramic capacitor.
A10	CNV+	DI	Conversion Start LVDS Input. A rising edge on CNV+ puts the internal sample-and-hold in hold mode and starts a conversion cycle. CNV+ can be also driven with a 2.5 V CMOS signal if CNV- is connected to GND.
B1	PDB_AMP	DI	Active Low. Connect this pin to GND to power down the fully differential ADC driver. Otherwise, connect this pin to VS+.
B8	TWOLANES	DI	Digital Input that Enables Two-Lane Output Mode. When TWOLANES is connected high (two-lane output mode), the ADAQ23876 outputs two bits at a time on DA-/DA+ and DB-/DB+. When TWOLANES is low (one-lane output mode), the ADAQ23876 outputs one bit at a time on DA-/DA+, and DB-/DB+ are disabled. Logic levels are determined by VIO.

## PIN CONFIGURATION AND FUNCTION DESCRIPTIONS

Table 6. Pin Function Descriptions (Continued)

Pin No.	Mnemonic	Type <sup>1</sup>	Description
B10	CNV-	DI	Conversion Start LVDS Input. A rising edge on CNV+ puts the internal sample-and-hold in hold mode and starts a conversion cycle. CNV+ can be also driven with a 2.5 V CMOS signal if CNV- is connected to GND.
C1, D1	OUT+	AO	Positive Output of the FDA.
C2, C4, E4, H1	VS+	P	FDA and Reference Buffer Positive Supply. The LDO output generating the VS+ supply of $\mu$ Module must be bypassed with at least 2.2 $\mu$ F (0402, X5R) ceramic capacitor to GND.
C3, D3	OUT-	AO	Negative Output of the FDA
C5, J1	VS-	P	FDA Negative Supply. Bypass this pin to GND with an at least 2.2 $\mu$ F (0402, X5R) ceramic capacitor.
D6	VCMO	AO	FDA Output Common-Mode Voltage. This pin is nominally REFBUF/2.
D10	CLK+	DI	LVDS Clock Input. This pin is an externally applied clock that serially shifts out the conversion result.
E10	CLK-	DI	LVDS Clock Input. This is an externally applied clock that serially shifts out the conversion result.
F1, F2	NC		No Connect.
G10	DCO+	DO	LVDS Data Clock Output. This is an echoed version of CLK+/CLK- that can be used to latch the data outputs.
H10	DCO-	DO	LVDS Data Clock Output. This is an echoed version of CLK+/CLK- that can be used to latch the data outputs.
J3, J4	REFBUF	AO	Reference Buffer Output Voltage. As a required component of SAR architecture, a 10 $\mu$ F ceramic bypass capacitor is already laid out within the ADAQ23876 between REFBUF and GND. Therefore, adding a second, smaller capacitor in parallel with the 10 $\mu$ F capacitor may degrade performance and is not recommended. The common-mode voltage of VCMO and LVDS pins are derived from the REFBUF. Therefore, a voltage at REFBUF pin must be stable after the ADAQ23876 is powered on or exits power-down mode before starting a conversion cycle.
J10	DA+	DO	Serial LVDS Data Output. In one-lane output mode, DB-/DB+ are not used and their LVDS driver is disabled to reduce power consumption.
K3	REFIN	P	Internal Reference Output/Reference Buffer Input. The output voltage of the internal reference, nominally 2.048 V, is output on this pin. An external reference can be applied to REFIN if a more accurate reference is required. If the internal reference buffer is not used, connect REFIN to GND to power down the buffer and connect an external buffered reference to REFBUF.
K5	PDB_ADC	DI	Digital Input that Enables the Power-Down Mode. When PDB_ADC is low, an internal ADC core enters power-down mode, and all circuitry (including the LVDS interface) is shutdown. When PDB_ADC is high, the device operates normally. Logic levels are determined by VIO.
K6	VDD	P	5 V Analog Power Supply. The range of VDD is 4.75 V to 5.25 V. Bypass the VDD pin to GND with an at least 2.2 $\mu$ F (0402, X5R) ceramic capacitor.
K7	TESTPAT	DI	Digital Input that Forces the LVDS Data Outputs to be a Test Pattern. When TESTPAT is high, the digital outputs are test pattern. When TESTPAT is low, the digital outputs are the ADAQ23876 conversion result. Logic levels are determined by VIO.
K8	DB-	DO	Serial LVDS Data Output. In one-lane output mode, DA-/DA+ are not used and their LVDS driver is disabled to reduce power consumption.
K9	DB+	DO	Serial LVDS Data Outputs. In one-lane output mode, DA-/DA+ are not used and their LVDS driver is disabled to reduce power consumption.
K10	DA-	DO	Serial LVDS Data Outputs. In one-lane output mode, DB-/DB+ are not used and their LVDS driver is disabled to reduce power consumption.

<sup>1</sup> AI is analog input, AO is analog output, P is power, DI is digital input, NC is no connection, and DO is digital output.

TYPICAL PERFORMANCE CHARACTERISTICS

VDD = 5 V ± 5%, VS+ = 5 V ± 5%, VS- = -1 V ± 5%, VS- = 0 V (95% of VIN), VIO = 2.375 V to 2.625 V, REFBUF = 4.096 V, sampling frequency (fs) = 15 MSPS, gain = 0.37, 0.73, 0.87, 1.38, and 2.25, and all specifications TMIN to TMAX, unless otherwise noted.

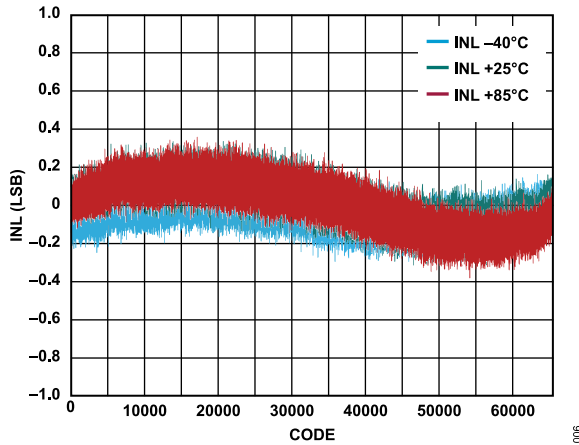


Figure 6. INL vs. Code for Various Temperatures, Gain = 2.25, Gain = 1.38, Gain = 0.87, Gain = 0.73, Differential, Single-Ended

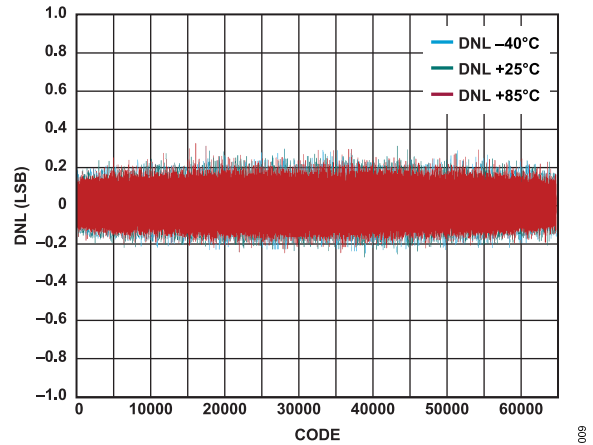


Figure 9. DNL vs. Code for Various Temperatures

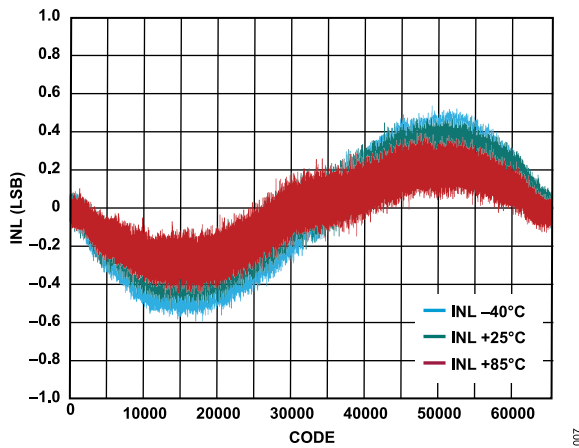


Figure 7. INL vs. Code for Various Temperatures, Gain = 0.37, Differential

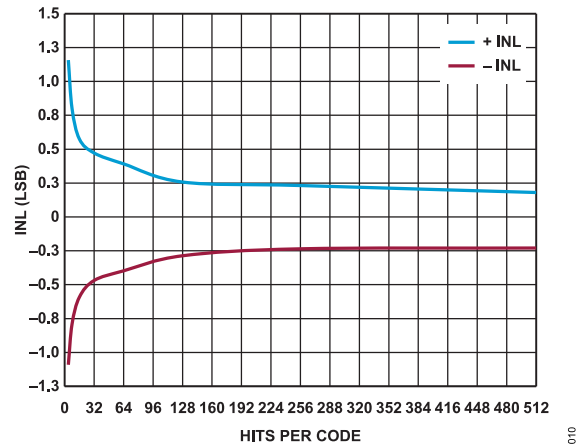


Figure 10. INL vs. Hits per Code, Gain = 2.25, Differential

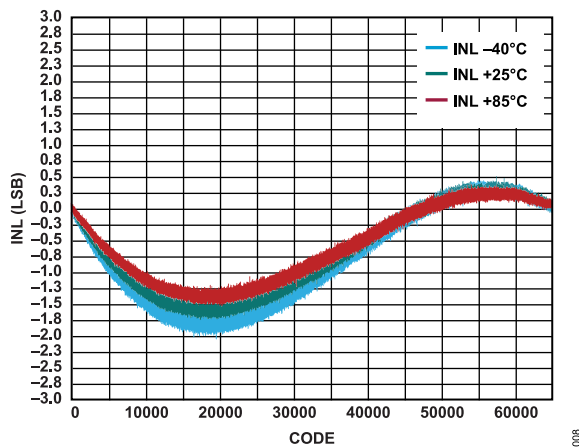


Figure 8. INL vs. Code for Various Temperatures, Gain = 0.37, Single-Ended

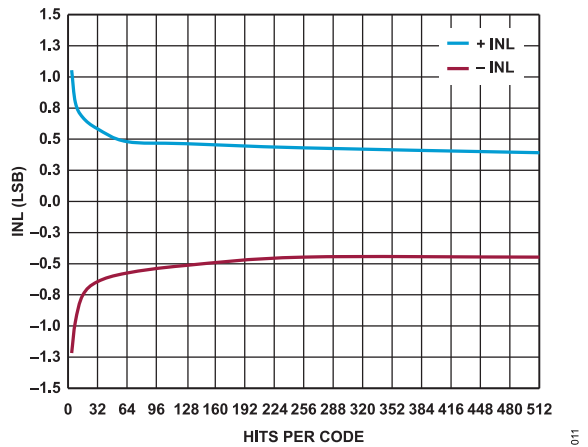


Figure 11. INL vs. Hits per Code, Gain = 0.37, Differential

TYPICAL PERFORMANCE CHARACTERISTICS

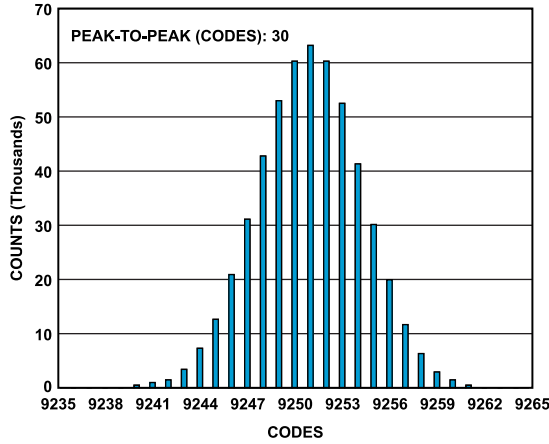


Figure 12. Histogram of a DC Input at the Code Transition

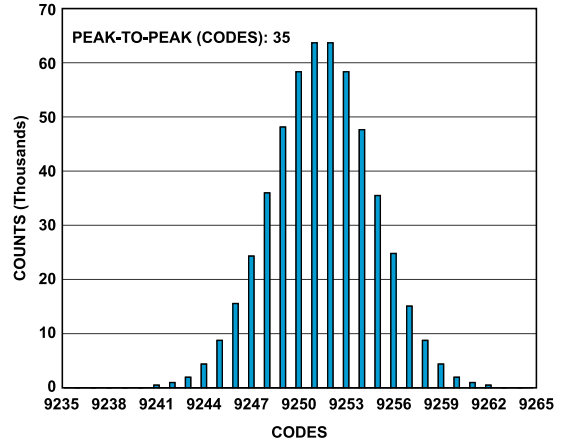


Figure 15. Histogram of a DC Input at the Code Center

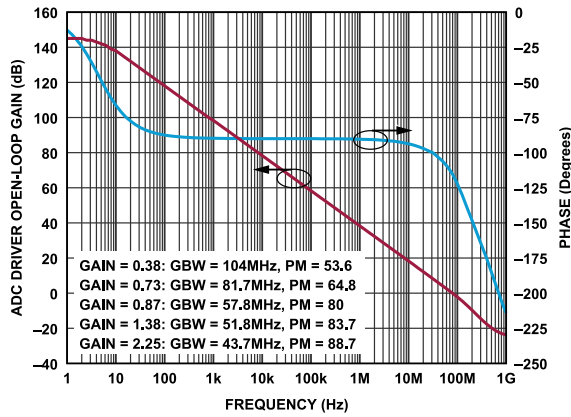


Figure 13. ADC Driver Open-Loop Gain and Phase vs. Frequency (GBW is Gain Bandwidth, PM is Phase Margin)

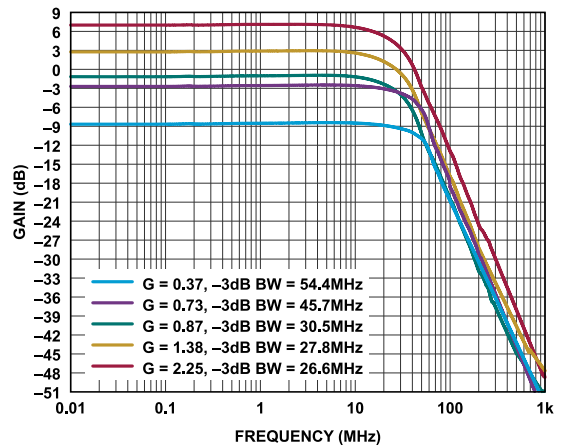


Figure 16. ADC Driver Frequency Response

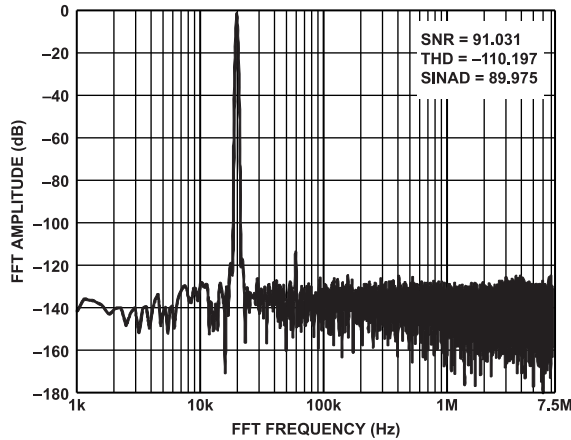


Figure 14. 20 kHz, -1 dBFS Input Tone FFT, Wide View, Gain = 0.37, Differential

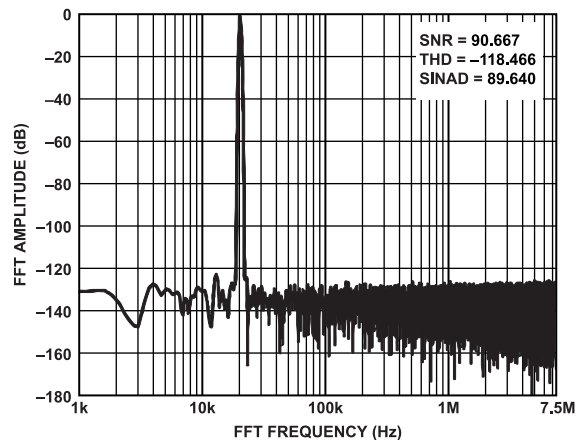


Figure 17. 20 kHz, -1 dBFS Input Tone FFT, Wide View, Gain = 0.73, Differential

TYPICAL PERFORMANCE CHARACTERISTICS

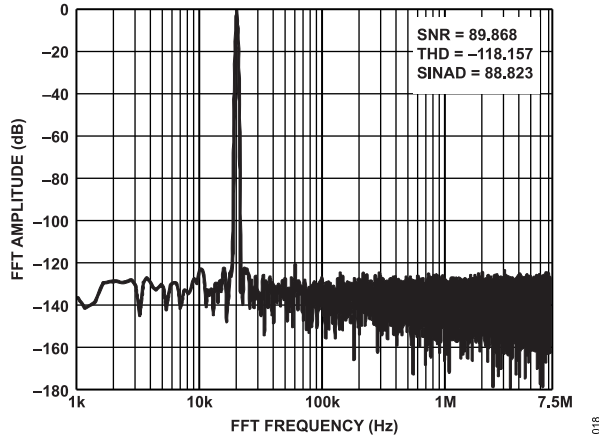


Figure 18. 20 kHz, -1 dBFS Input Tone FFT, Wide View, Gain = 0.87, Differential

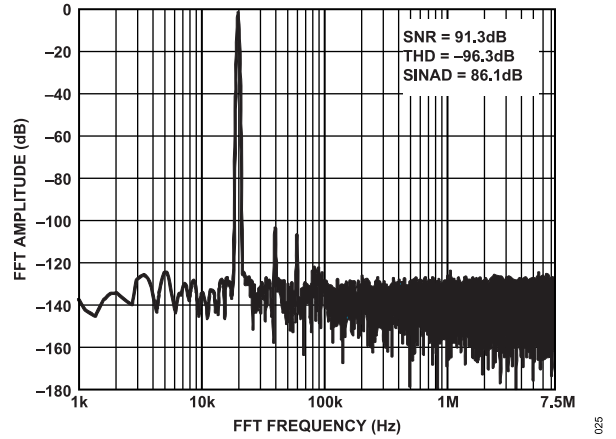


Figure 21. 20 kHz, -1 dBFS Input Tone FFT, Wide View, Gain = 0.37, Single-Ended, VICM = 0 V

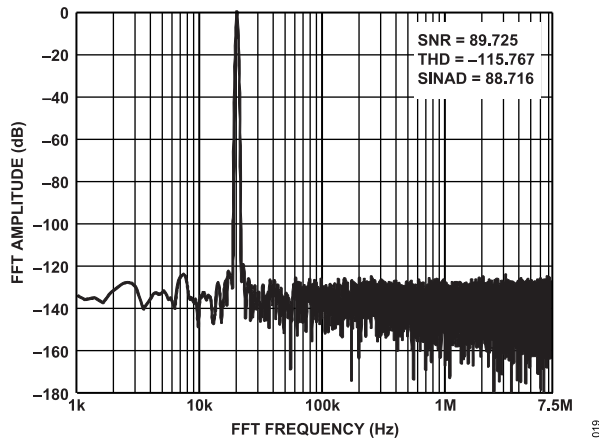


Figure 19. 20 kHz, -1 dBFS Input Tone FFT, Wide View, Gain = 1.38, Differential

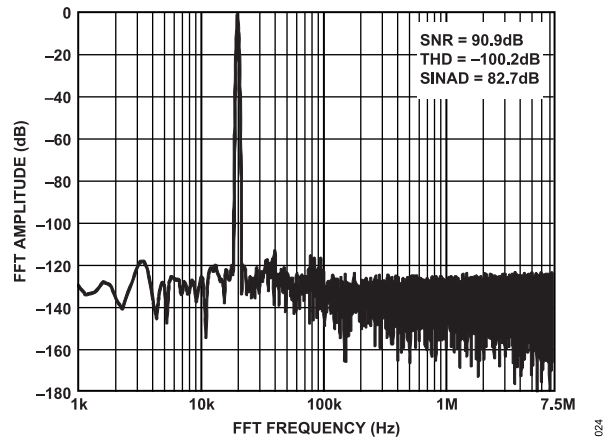


Figure 22. 20 kHz, -1 dBFS Input Tone FFT, Wide View, Gain = 0.73, Single-Ended, VICM = 0 V

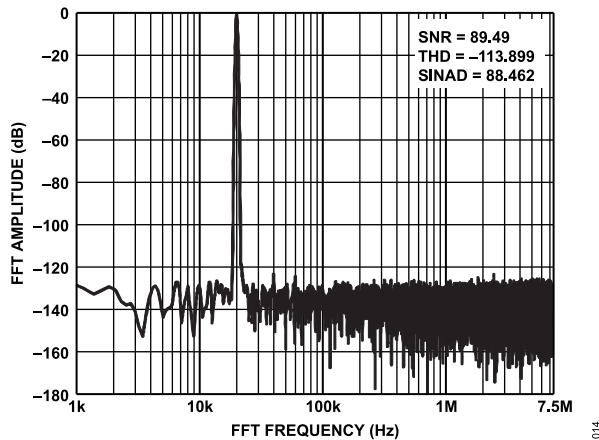


Figure 20. 20 kHz, -1 dBFS Input Tone FFT, Wide View, Gain = 2.25, Differential

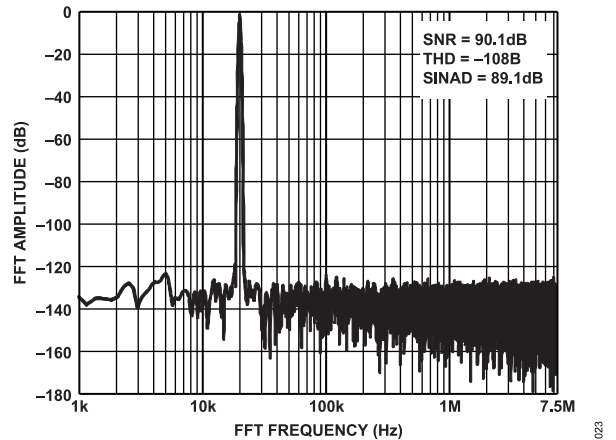


Figure 23. 20 kHz, -1 dBFS Input Tone FFT, Wide View, Gain = 0.87, Single-Ended, VICM = 0 V

TYPICAL PERFORMANCE CHARACTERISTICS

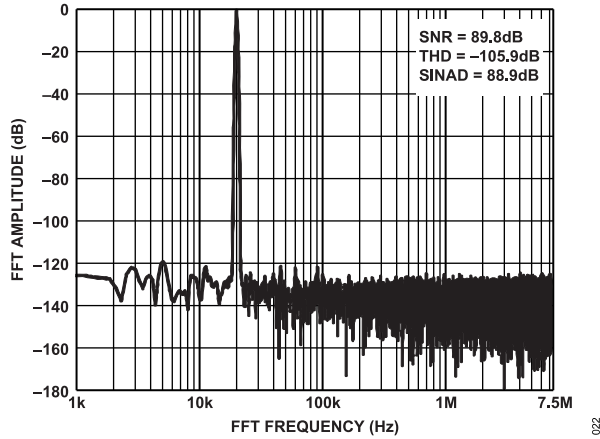


Figure 24. 20 kHz, -1 dBFS Input Tone FFT, Wide View, Gain = 1.38, Single-Ended, VICM = 0 V

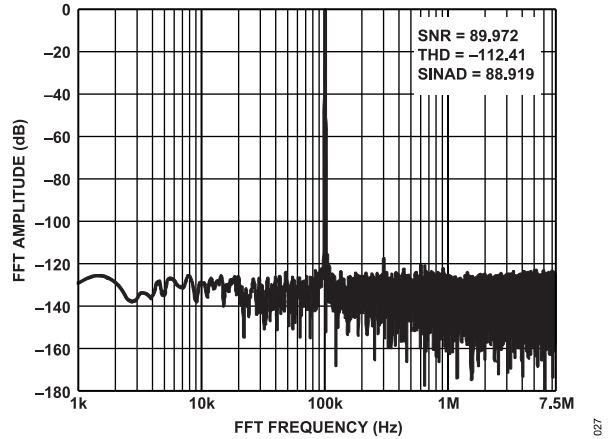


Figure 27. 100 kHz, -1 dBFS Input Tone FFT, Wide View, Gain = 0.73, Differential

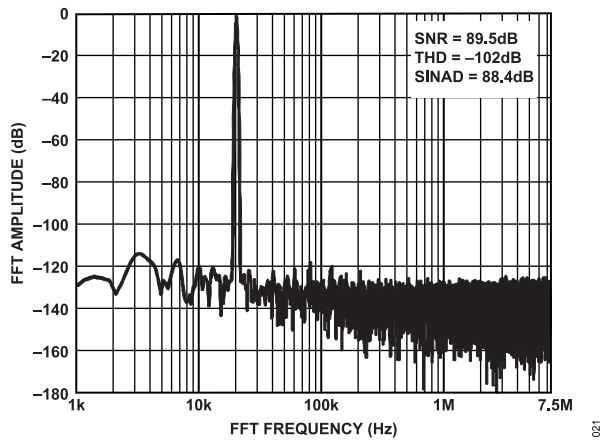


Figure 25. 20 kHz, -1 dBFS Input Tone FFT, Wide View, Gain = 2.25, Single-Ended, VICM = 0 V

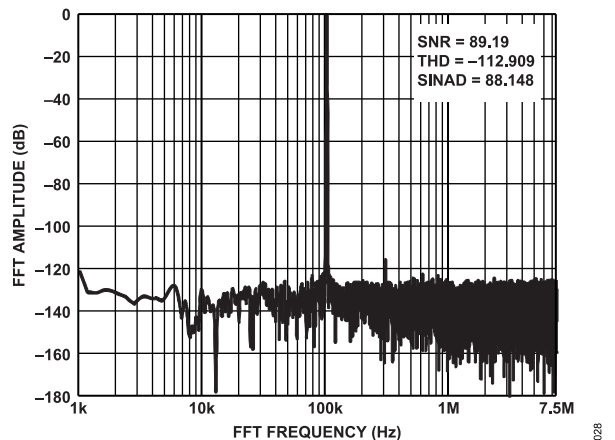


Figure 28. 100 kHz, -1 dBFS Input Tone FFT, Wide View, Gain = 0.87, Differential

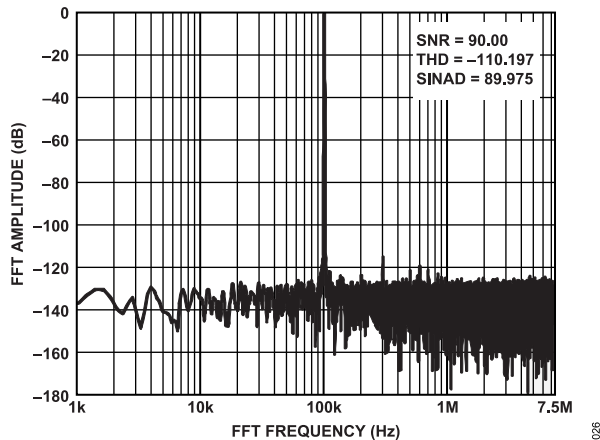


Figure 26. 100 kHz, -1 dBFS Input Tone FFT, Wide View, Gain = 0.37, Differential

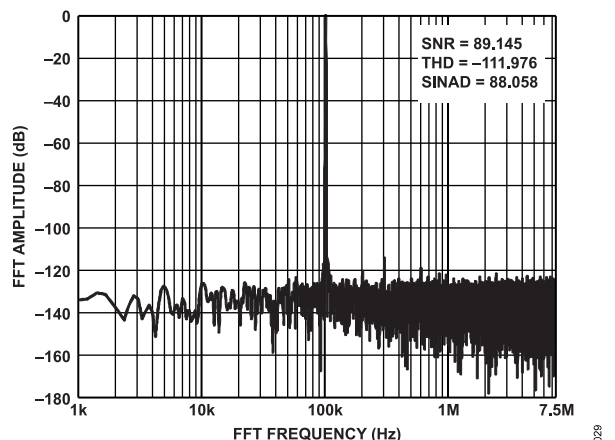


Figure 29. 100 kHz, -1 dBFS Input Tone FFT, Wide View, Gain = 1.38, Differential

TYPICAL PERFORMANCE CHARACTERISTICS

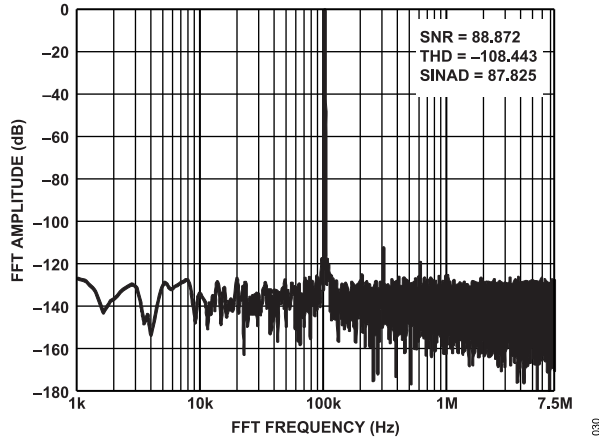


Figure 30. 100 kHz, -1 dBFS Input Tone FFT, Wide View, Gain = 2.25, Differential

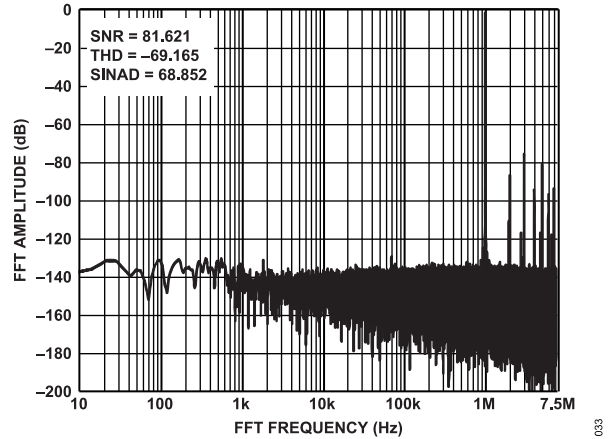


Figure 33. 1 MHz, -1 dBFS Input Tone FFT, Wide View, Gain = 1.38, Differential

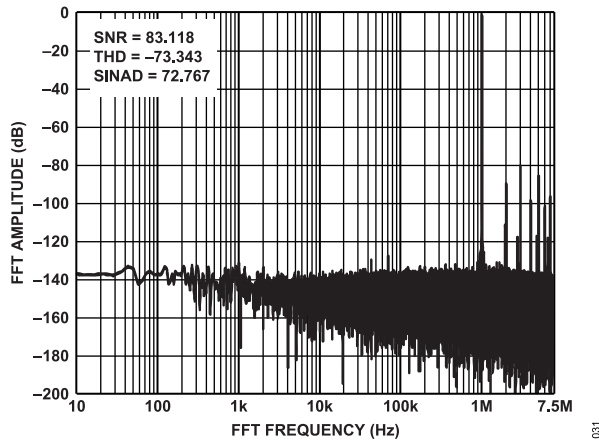


Figure 31. 1 MHz, -1 dBFS Input Tone FFT, Wide View, Gain = 0.73, Differential

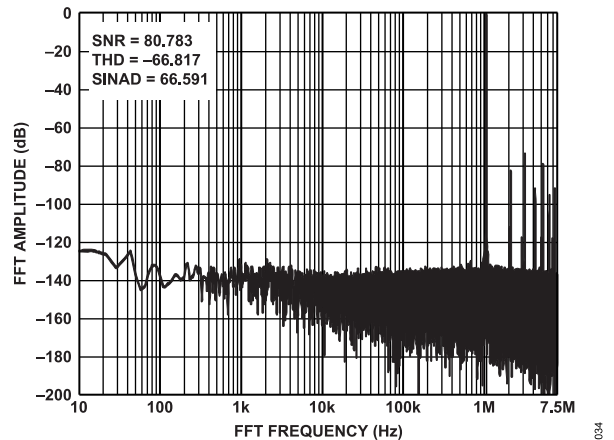


Figure 34. 1 MHz, -1 dBFS Input Tone FFT, Wide View, Gain = 2.25, Differential

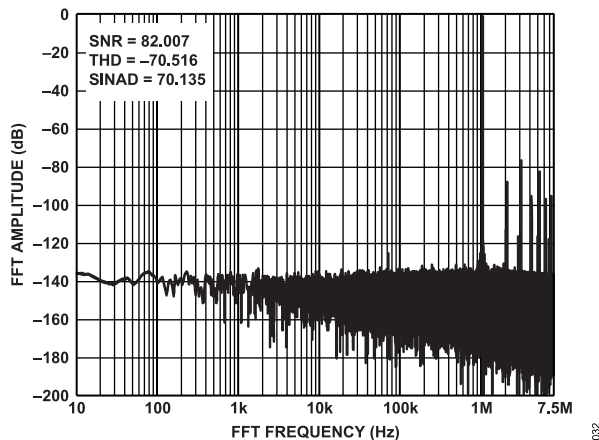


Figure 32. 1 MHz, -1 dBFS Input Tone FFT, Wide View, Gain = 0.87, Differential

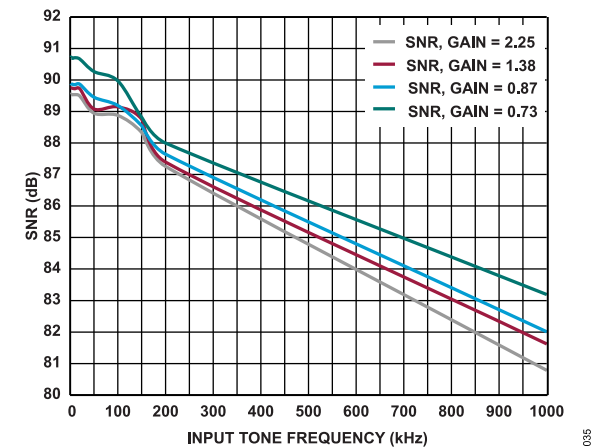


Figure 35. SNR vs. Input Tone Frequency, Gain = 0.73, Gain = 0.87, Gain = 1.38, and Gain = 2.25

TYPICAL PERFORMANCE CHARACTERISTICS

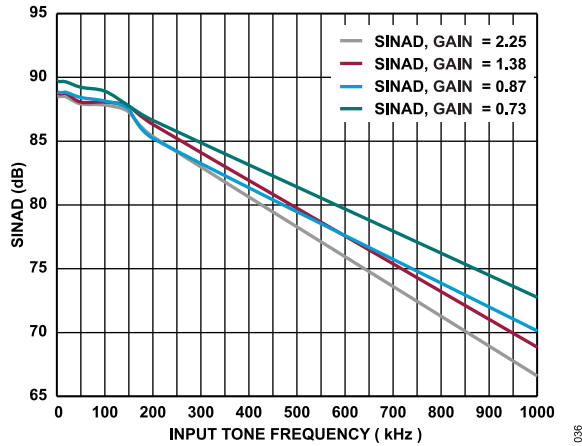


Figure 36. SINAD vs. Input Tone Frequency, Gain = 0.73, Gain = 0.87, Gain = 1.38, Gain = 2.25

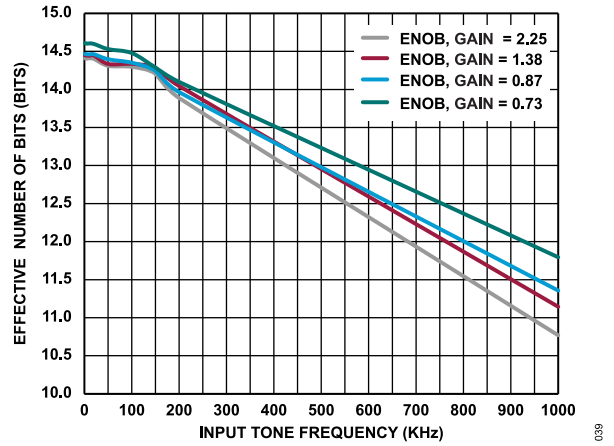


Figure 39. Effective Number of Bits vs. Input Tone Frequency, Gain = 0.73, Gain = 0.87, Gain = 1.38, and Gain = 2.25

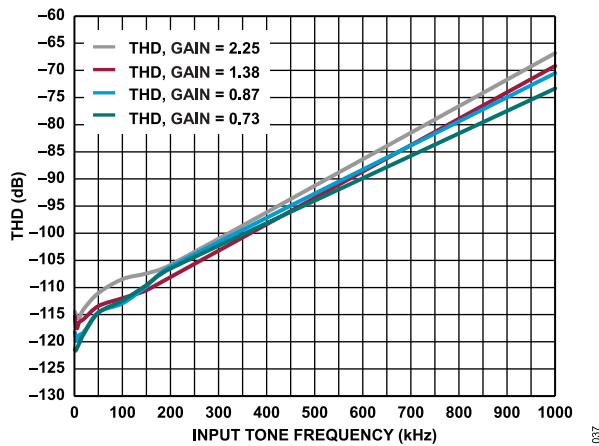


Figure 37. THD vs. Input Tone Frequency, Gain = 0.73, Gain = 0.87, Gain = 1.38, Gain = 2.25

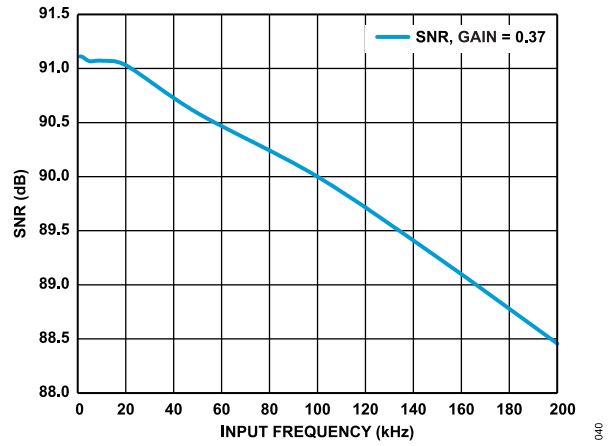


Figure 40. SNR vs. Input Frequency, Gain = 0.37

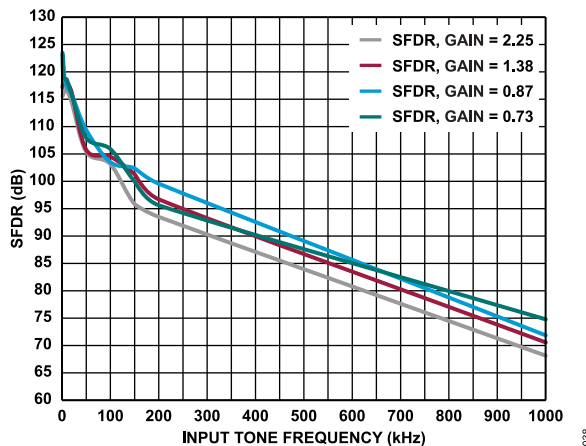


Figure 38. SFDR vs. Input Tone Frequency, Gain = 0.73, Gain = 0.87, Gain = 1.38, and Gain = 2.25

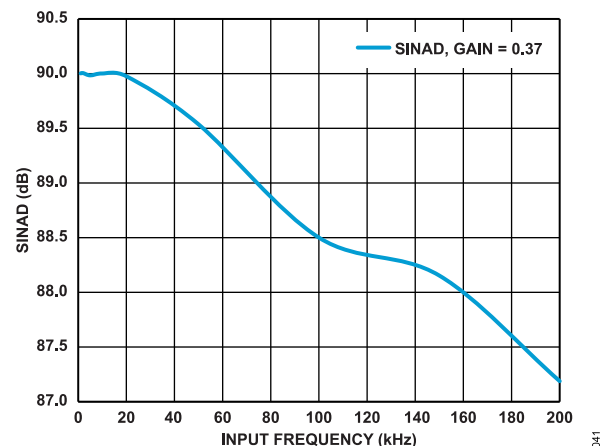


Figure 41. SINAD vs. Input Frequency, Gain = 0.37

TYPICAL PERFORMANCE CHARACTERISTICS

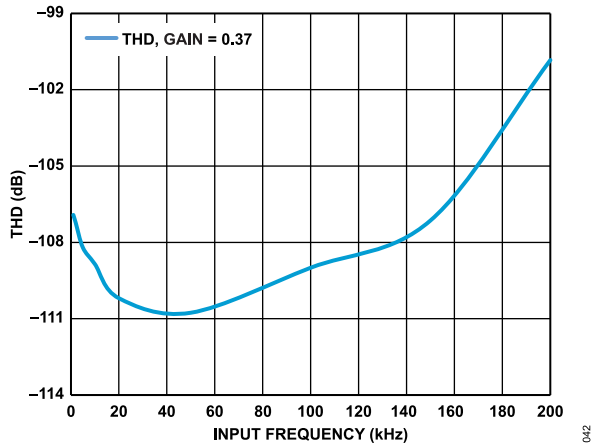


Figure 42. THD vs. Input Frequency, Gain = 0.37

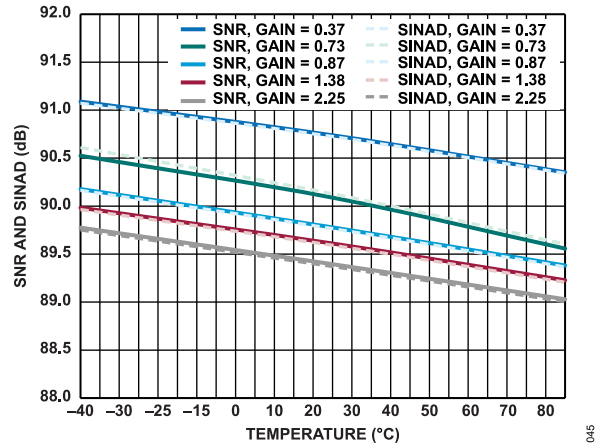


Figure 45. SNR and SINAD vs. Temperature, Gain,  $f_{IN} = 1$  kHz

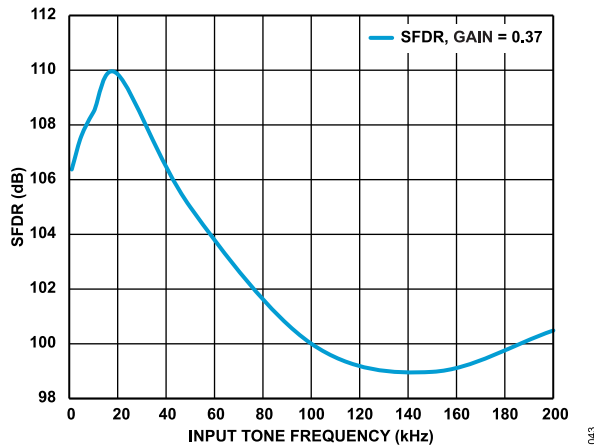


Figure 43. SFDR vs. Input Tone Frequency, Gain = 0.37

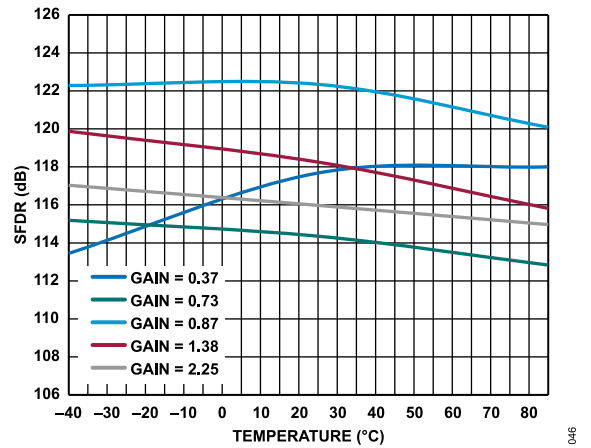


Figure 46. SFDR vs. Temperature, Gain,  $f_{IN} = 1$  kHz

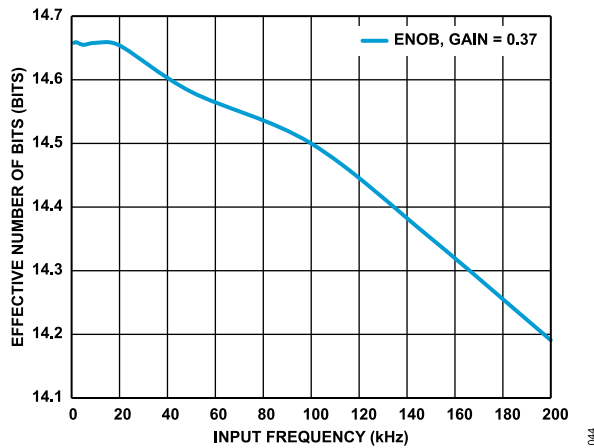


Figure 44. Effective Number of Bits vs. Input Frequency, Gain = 0.37

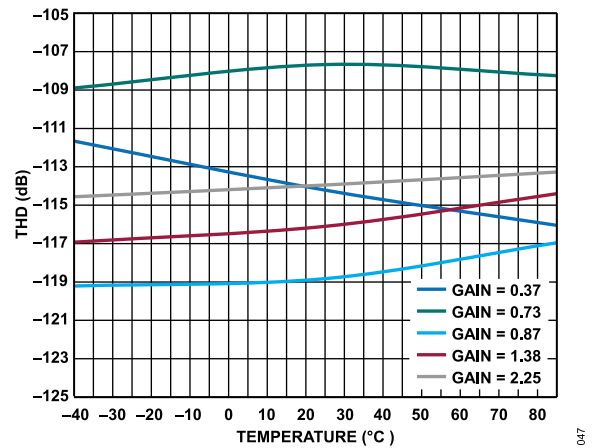


Figure 47. THD vs. Temperature, Gain,  $f_{IN} = 1$  kHz

TYPICAL PERFORMANCE CHARACTERISTICS

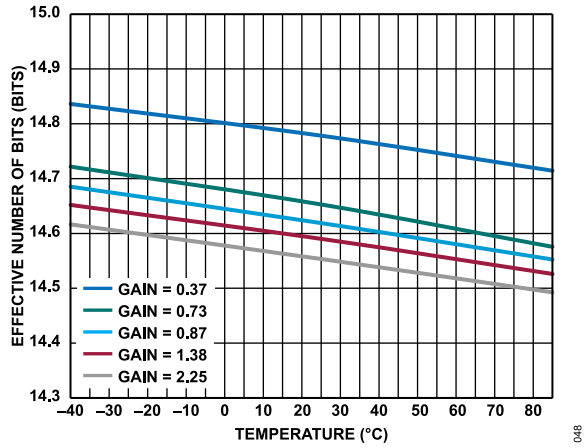


Figure 48. Effective Number of Bits vs. Temperature, Gain,  $f_{IN} = 1 \text{ kHz}$

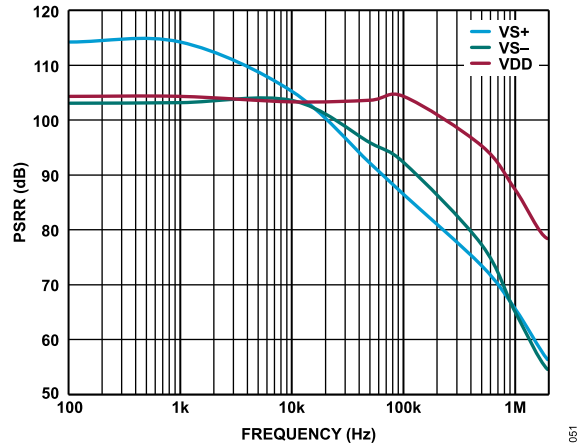


Figure 51. PSRR vs. Frequency

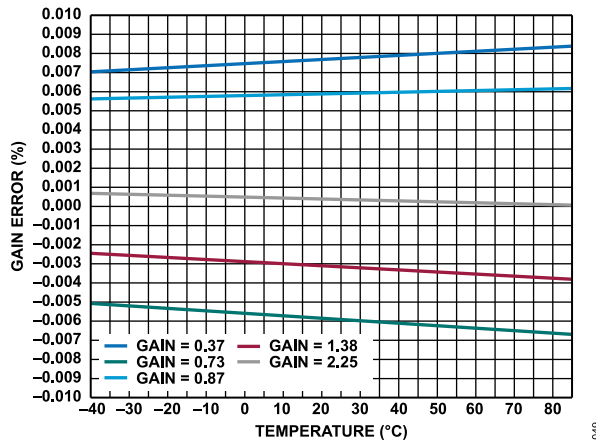


Figure 49. Gain Error vs. Temperature

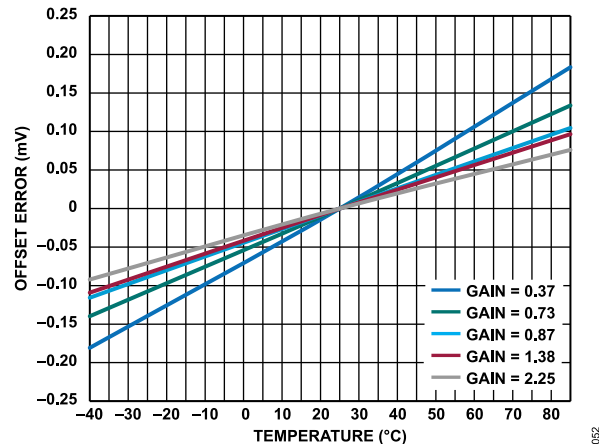


Figure 52. Offset Error vs. Temperature

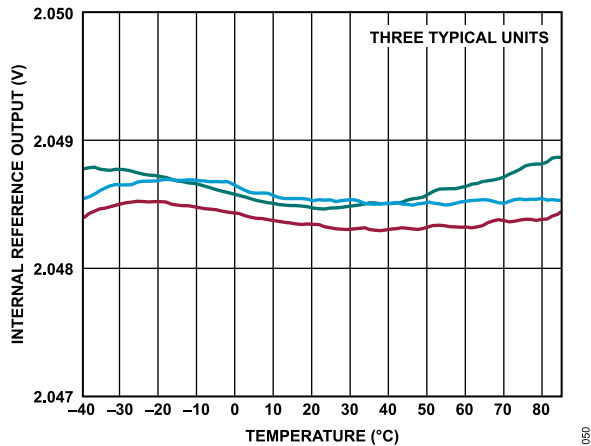


Figure 50. Internal Reference Output vs. Temperature

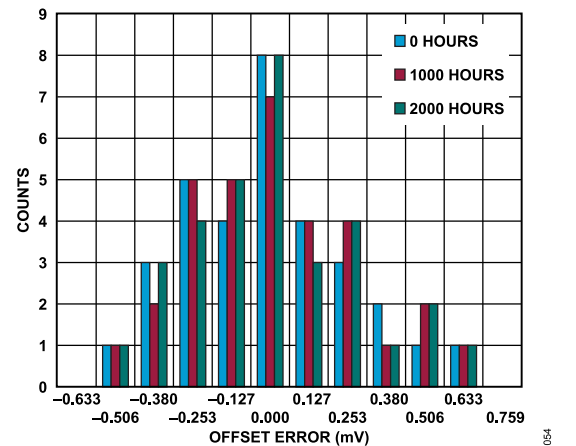


Figure 53. Long Term Drift Offset Error, Gain = 1.38

TYPICAL PERFORMANCE CHARACTERISTICS

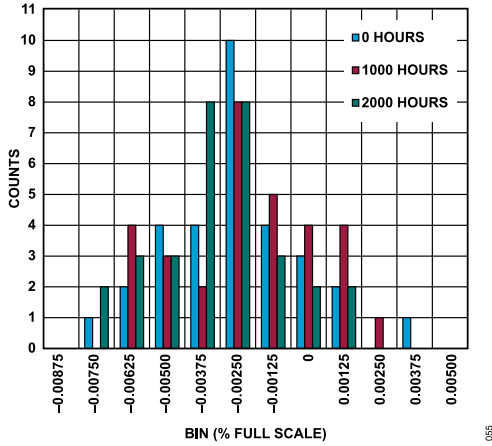


Figure 54. Long Term Drift Gain Error, Gain = 0.37

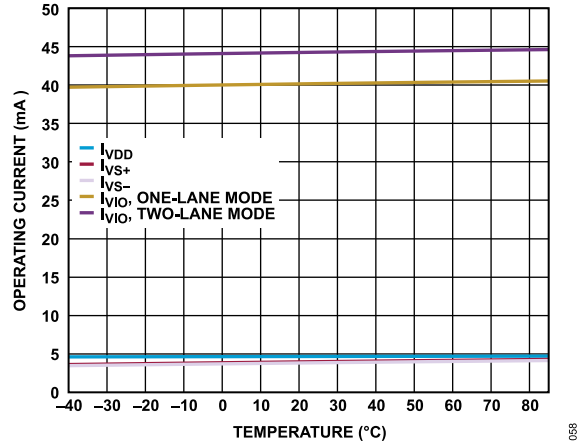


Figure 57. Operating Current vs. Temperature ( $I_{VDD}$  = VDD Current,  $I_{VS+}$  = VS+ Current,  $I_{VS-}$  = VS- Current,  $I_{VIO}$  = VIO Current)

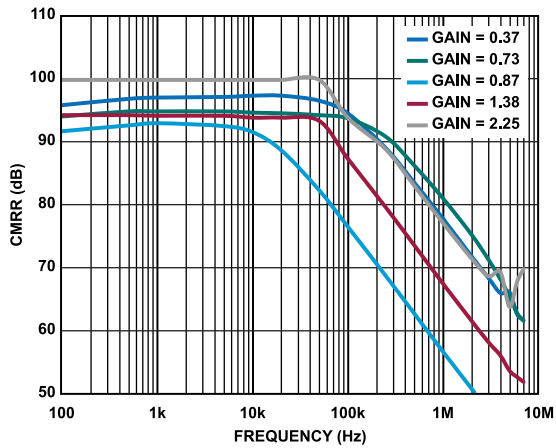


Figure 55. CMRR vs. Frequency

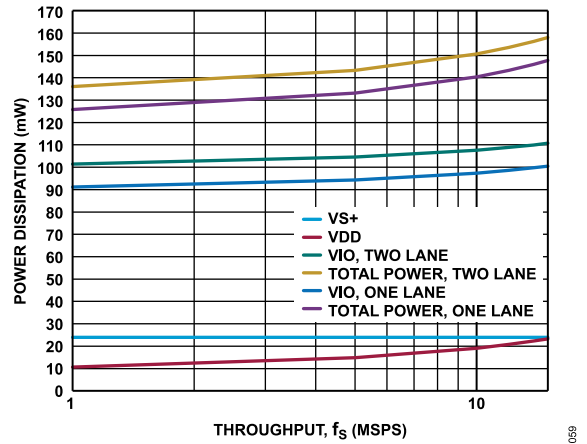


Figure 58. Power Dissipation vs. Throughput, 25°C

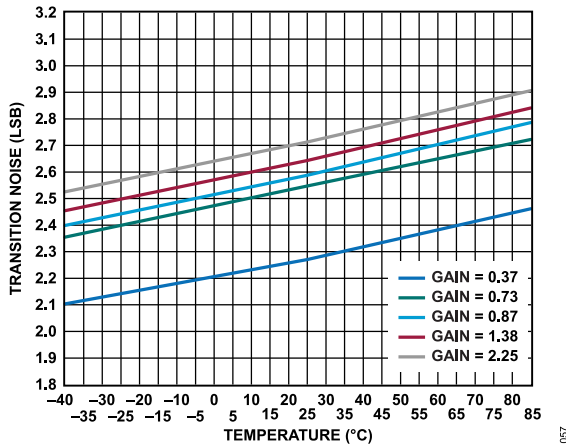


Figure 56. Transition Noise vs. Temperature, Gain

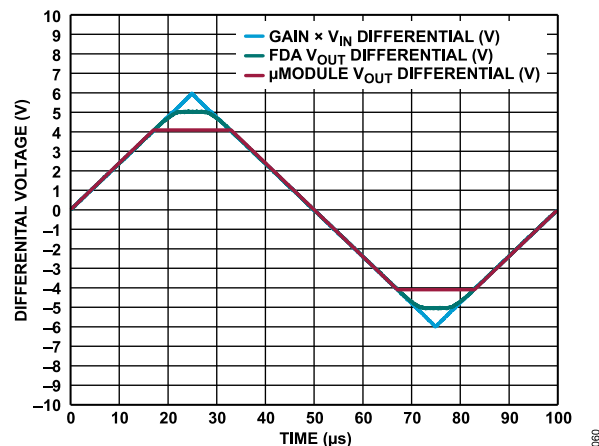


Figure 59. Differential Voltage vs. Time,  $f_{IN}$  = 10 kHz

TYPICAL PERFORMANCE CHARACTERISTICS

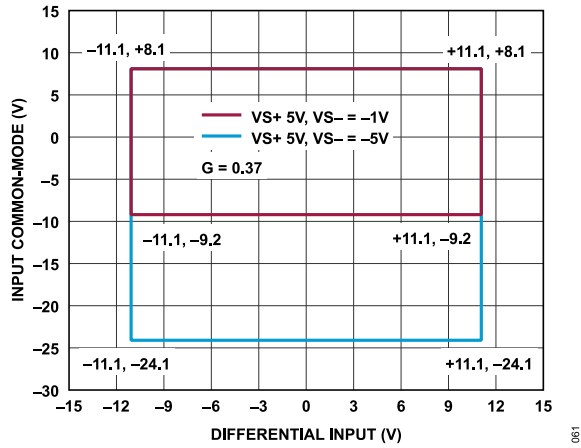


Figure 60. Input Common-Mode Voltage vs. Differential Input Voltage, Gain = 0.37

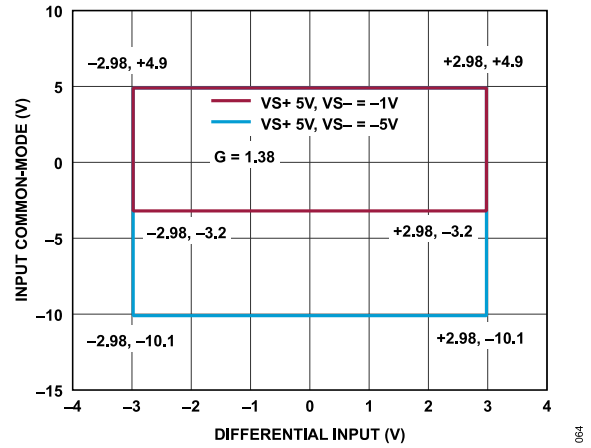


Figure 63. Input Common-Mode Voltage vs. Differential Input Voltage, Gain = 1.38

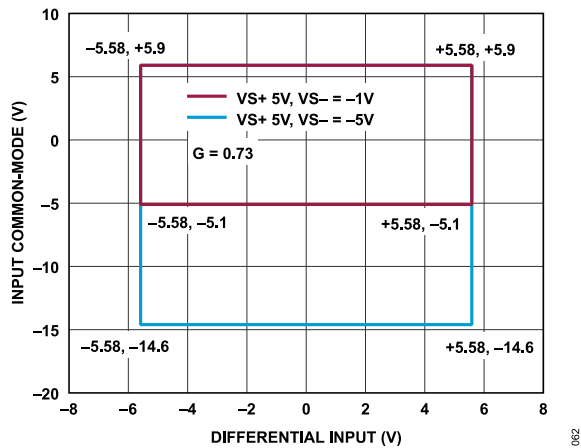


Figure 61. Input Common-Mode Voltage vs. Differential Input Voltage, Gain = 0.73

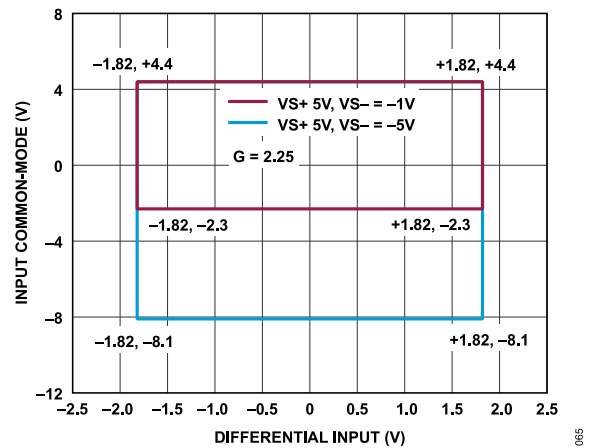


Figure 64. Input Common-Mode Voltage vs. Differential Input Voltage, Gain = 2.25

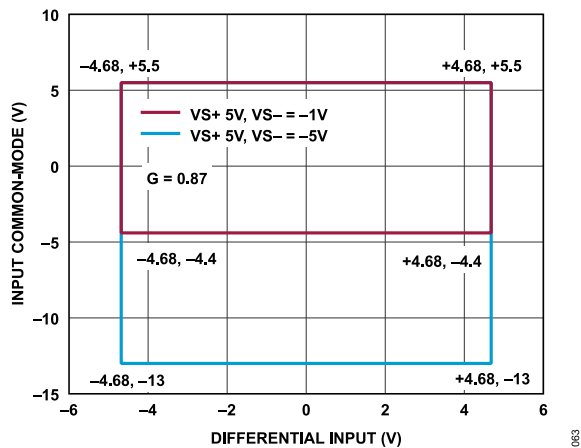


Figure 62. Input Common-Mode Voltage vs. Differential Input Voltage, Gain = 0.87

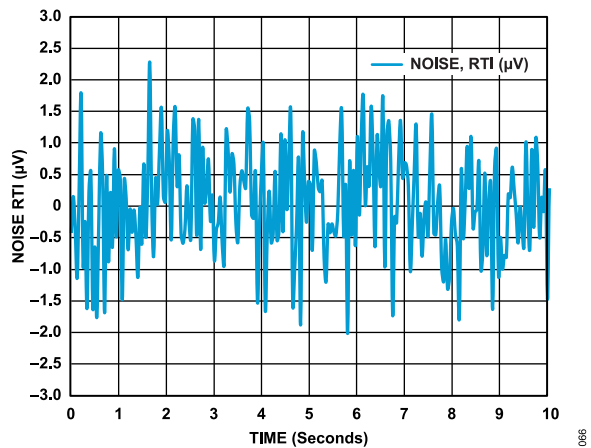


Figure 65. Voltage Noise for 0.1 Hz to 10 Hz Bandwidth,  $f_s = 100$  kSPS, 256 Samples Averaged per Reading, OSR = 4096

TYPICAL PERFORMANCE CHARACTERISTICS

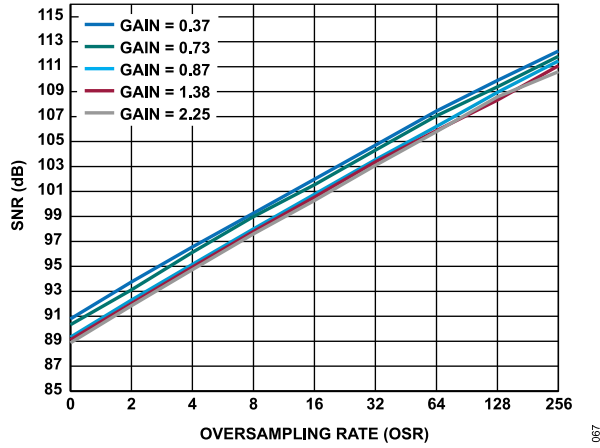


Figure 66. SNR vs. Oversampling Rate for Input Frequencies,  $f_{IN} = 1$  kHz

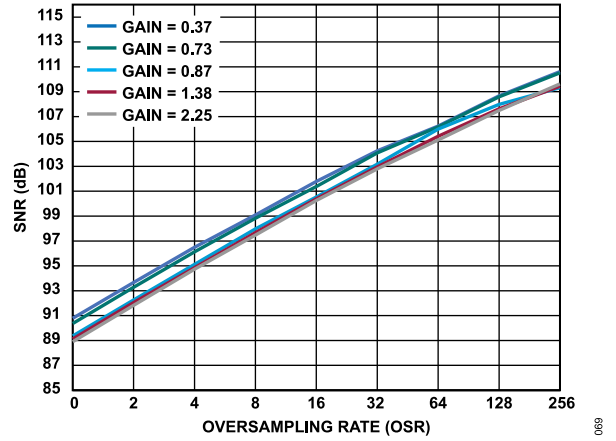


Figure 68. SNR vs. Oversampling Rate for Input Frequencies,  $f_{IN} = 10$  kHz

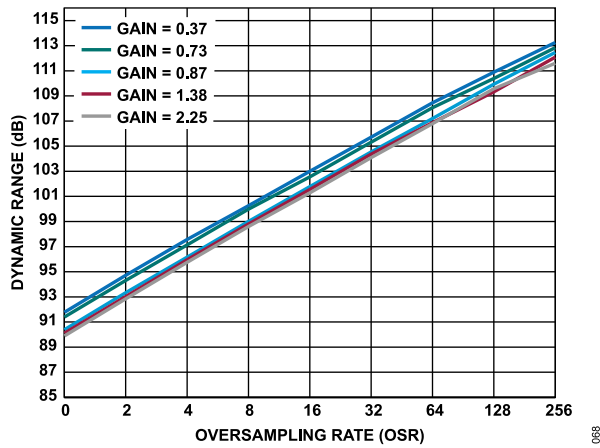


Figure 67. Dynamic Range vs. Oversampling Rate

## TERMINOLOGY

### Integral Nonlinearity (INL)

INL is the deviation of each individual code from a line drawn from negative full scale through positive full scale. The point used as negative full scale occurs ½ LSB before the first code transition. Positive full scale is defined as a level 1½ LSB beyond the last code transition. The deviation is measured from the middle of each code to the true straight line.

### Differential Nonlinearity (DNL)

In an ideal  $\mu$ Module, code transitions are 1 LSB apart. DNL is the maximum deviation from this ideal value. It is often specified in terms of resolution for which no missing codes are guaranteed.

### Offset Error

The first transition occurs at a level ½ LSB above analog ground (62.5  $\mu$ V for the gain = 1.38,  $\pm 2.5$  V range). Offset error is the difference between the ideal midscale input voltage (0 V) and the actual voltage producing the midscale output code.

### Offset Error Drift

Drift offset error drift is the ratio of the offset error change due to a temperature change of 1°C and the full-scale code range (gain = 1.38,  $\pm 2.5$  V range). This drift is expressed in parts per million per degree Celsius as follows:

$$\text{Offset Error Drift (ppm/}^\circ\text{C)} = 10^6 \times (\text{Offset Error}_{T_{MAX}} - \text{Offset Error}_{T_{MIN}}) / (T_{MAX} - T_{MIN})$$

where:  $T_{MAX} = 85^\circ\text{C}$  and  $T_{MIN} = -40^\circ\text{C}$ .

### Gain Error

The first transition (from 100...000 to 1000...001) occurs at a level ½ LSB above nominal negative full scale and the last transition (from 011...110 to 011...111) occurs for an analog voltage 1½ LSB below the nominal positive full scale. The gain error is the deviation of the difference between the actual level of the last transition and the actual level of the first transition from the ideal levels after the offset error is removed. In addition, the absolute accuracy of the reference used for the  $\mu$ Module can be a large source of error. Therefore, this error source is removed by measuring its value and using it to determine positive full scale (PFS) and negative full scale (NFS) for the gain error calculation. If the reference used cannot be measured, its deviation from ideal must be factored into the gain error calculation.

This error is expressed in percentage as follows:

$$\text{Gain Error}(\%) = 100 \times ((\text{PFS} - \text{NFS})_{ACTUAL\_CODE} - (\text{PFS} - \text{NFS})_{IDEAL\_CODE}) / (\text{PFS} - \text{NFS})_{IDEAL\_CODE}$$

where:

PFS is positive full scale.

NFS is negative full scale.

### Gain Error Drift

Gain error drift is the ratio of the gain error change due to a temperature change of 1°C and the full-scale range (gain = 0.37,  $\pm 10$  V range). This drift is expressed in parts per million per degree Celsius as follows:

$$\text{Gain Error Drift (ppm/}^\circ\text{C)} = 10^6 \times (\text{Gain Error}_{T_{MAX}} - \text{Gain Error}_{T_{MIN}}) / (T_{MAX} - T_{MIN})$$

where:  $T_{MAX} = 85^\circ\text{C}$  and  $T_{MIN} = -40^\circ\text{C}$ .

### Spurious-Free Dynamic Range (SFDR)

SFDR is defined as the difference, in dB, between the peak spurious or harmonic component in the ADC output spectrum (up to  $f_s/2$  and excluding dc) and the rms value of the fundamental.

### Effective Number of Bits (ENOB)

ENOB is a measurement of the resolution with a sine wave input. ENOB is related to SINAD and expressed in bits as follows:

$$\text{ENOB} = (\text{SINAD}_{dB} - 1.76) / 6.02$$

### Total Harmonic Distortion (THD)

THD is the ratio of the rms sum of the first five harmonic components to the rms value of a full-scale input signal and is expressed in decibels.

### Dynamic Range

Dynamic range is the ratio of the rms value of the full scale to the total rms noise measured. The value for dynamic range is expressed in decibels. It is measured with a signal at  $-60$  dBFS so that it includes all noise sources and DNL artifacts.

### Signal-to-Noise Ratio (SNR)

SNR is the ratio of the rms value of the actual input signal to the rms sum of all other spectral components below the Nyquist frequency, excluding harmonics and dc. The value for SNR is expressed in decibels.

### Signal-to-Noise-and-Distortion (SINAD) Ratio

SINAD is the ratio of the rms value of the actual input signal to the rms sum of all other spectral components that are less than the Nyquist frequency, including harmonics but excluding dc. The value of SINAD is expressed in decibels.

### Aperture Delay

Aperture delay is the measure of the acquisition performance and is the time between the rising edge of the CNV input and when the input signal is held for a conversion.

### Transient Response

Transient response is the time required for the  $\mu$ Module to acquire a full-scale input step to  $\pm 1$  LSB accuracy.

**TERMINOLOGY****Common-Mode Rejection Ratio (CMRR)**

CMRR is the ratio of the power in the  $\mu$ Module output at the frequency,  $f$ , to the power of a 1.3 V p-p sine wave applied to the input common-mode voltage of frequency,  $f$ .

$$CMRR \text{ (dB)} = 10 \log(P_{\mu\text{Module\_IN}}/P_{\mu\text{Module\_OUT}})$$

where:

$P_{\mu\text{Module\_IN}}$  is the common-mode power at the frequency,  $f$ , applied to the inputs.

$P_{\mu\text{Module\_OUT}}$  is the power at the frequency,  $f$ , in the  $\mu$ Module output.

**Power Supply Rejection Ratio (PSRR)**

PSRR is the ratio of the power in the  $\mu$ Module output at the frequency,  $f$ , to the power of a 500 mV p-p sine wave applied to the VDD and VS+ supply voltage centered at 5 V and 100 mV p-p for a VS- supply voltage centered at -1 V of frequency,  $f$ .

$$PSRR \text{ (dB)} = 10 \log(P_{\mu\text{Module\_IN}}/P_{\mu\text{Module\_OUT}})$$

where:

$P_{\mu\text{Module\_IN}}$  is the power at the frequency,  $f$ , at each of the VDD, VS+, and VS- supply pins.

$P_{\mu\text{Module\_OUT}}$  is the power at the frequency,  $f$ , in the  $\mu$ Module output.

THEORY OF OPERATION

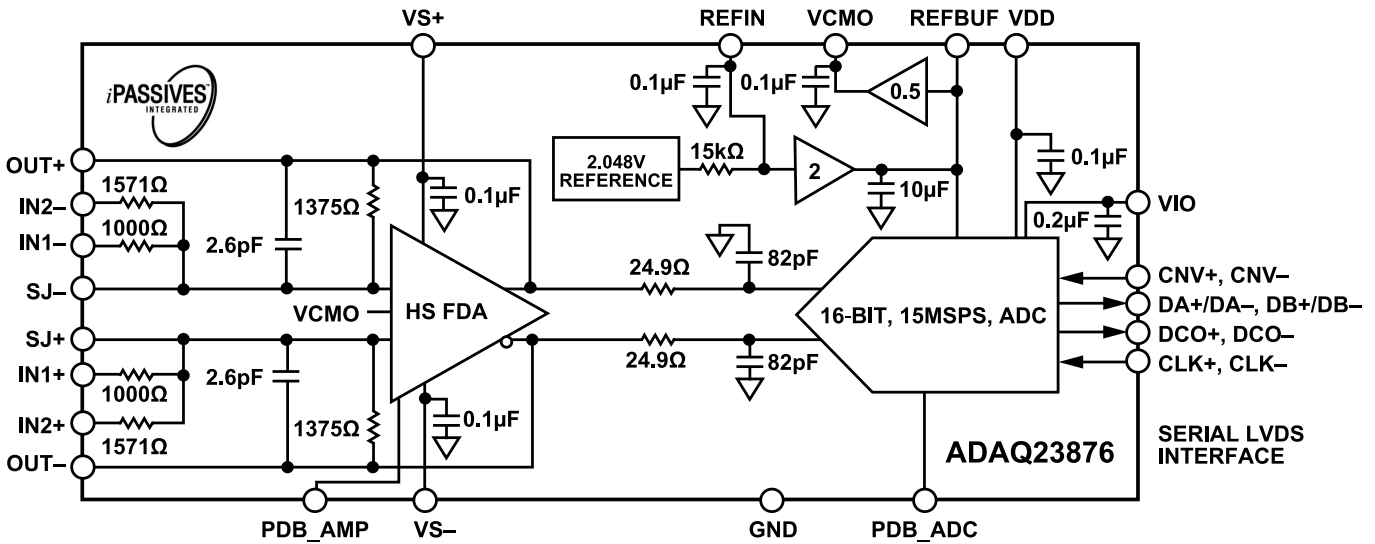


Figure 69. ADAQ23876 μModule Simplified Block Diagram

CIRCUIT INFORMATION

The ADAQ23876 is a precision, high speed, μModule data acquisition solution that reduces the development cycle of precision measurement systems by transferring the design burden of component selection, optimization, and layout from the designer to the device. The ADAQ23876 reduces the end system component count by combining multiple common signal processing and conditioning blocks in a single device, including a low noise, fully differential ADC driver, a stable reference buffer, and a high speed, 16-bit, 15 MSPS SAR ADC. The device also incorporates the Analog Devices proprietary iPassives technology components necessary for optimum performance. The superior matching and drift characteristics of the resistors minimizes temperature dependent error sources.

The ADAQ23876 includes a precision internal 2.048 V reference, as well as an internal reference buffer. The ADAQ23876 also has a high speed serial LVDS interface that can output one or two bits at a time. The fast 15 MSPS throughput with no pipeline latency makes the ADAQ23876 ideally suited for a wide variety of high speed applications. The ADAQ23876 dissipates only 143 mW at 15 MSPS.

TRANSFER FUNCTION

The ADAQ23876 μModule digitizes the full-scale voltage of  $2 \times V_{REF}$  in to  $2^{16}$  levels, resulting in an LSB size of 125 μV with  $REFBUF = 4.096$  V. The output data is in twos complement format. The ideal transfer function is shown in Figure 70. The ideal offset binary transfer function can be obtained from the twos complement transfer function by inverting the MSB of each output code.

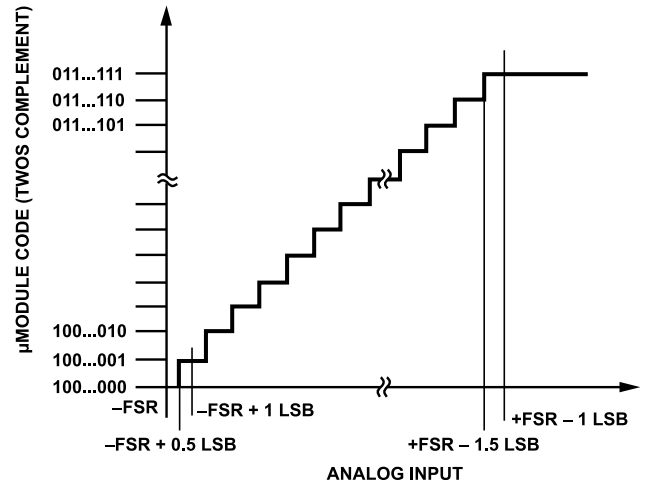


Figure 70. ADAQ23876 Transfer Function (FSR Is Full-Scale Range)

Table 7. Output Codes and Ideal Input Voltages

Description	Inputs Voltages	Digital Output Code (Twos Complement, Hex)
FSR - 1 LSB	$(32,767 \times V_{REF}) / (32,768 \times \text{gain})$	0x7FFF
Midscale + 1 LSB	$V_{REF} / (32,768 \times \text{gain})$	0x0001
Midscale	0 V	0x0000
Midscale - 1 LSB	$-V_{REF} / (32,768 \times \text{gain})$	0xFFFF
-FSR + 1 LSB	$-(32,767 \times V_{REF}) / (32,768 \times \text{gain})$	0x8001
-FSR	$-V_{REF} / \text{gain}$	0x8000

APPLICATIONS INFORMATION

TYPICAL APPLICATION DIAGRAMS

Figure 71 to Figure 75 shows the typical application examples of differential signals applied to each of the ADAQ23876 inputs for a given gain with varying common-mode voltages. Figure 76 to Figure 80 shows the typical application example of a single-ended

signal applied to one of the ADAQ23876 inputs for a given gain with a fixed common-mode voltage of 0 V.

Table 8 shows how to apply the input signal for a given gain or input range option.

Table 8. Gain Configuration and Input Range

Gain	Input Range	Input Signal on Pins	Test Conditions
0.37	$\pm 10$ V	IN2+, IN2-	Connect the OUT+, IN1-, OUT-, and IN1+ pins together (see Figure 71 and Figure 76)
0.73	$\pm 5$ V	IN1+, IN1-	Connect the OUT+, IN2-, OUT-, and IN2+ pins together (see Figure 72 and Figure 77)
0.87	$\pm 4.096$ V	IN2+, IN2-	Leave the IN1+ and IN1- pins floating (see Figure 73 and Figure 78)
1.38	$\pm 2.5$ V	IN1+, IN1-	Leave the IN2+ and IN2- pins floating (see Figure 74 and Figure 78)
2.25	$\pm 1.5$ V	IN2+/IN1+, IN2-/IN1-	Connect the IN2-, IN1-, IN2+, and IN1+ pins together (see Figure 75 and Figure 80)

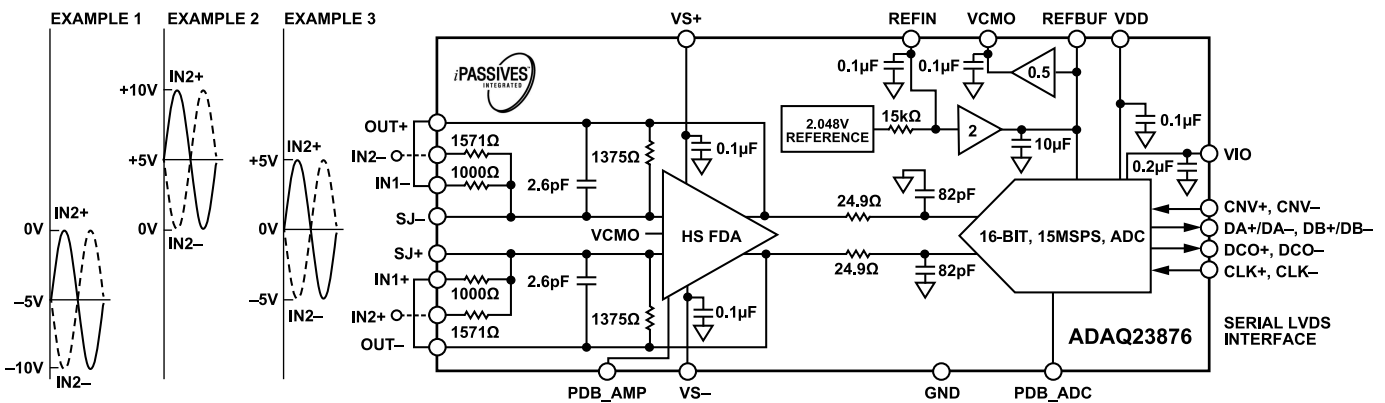


Figure 71. ADAQ23876 Differential Input Configuration with Gain = 0.37,  $\pm 10$  V Input Range

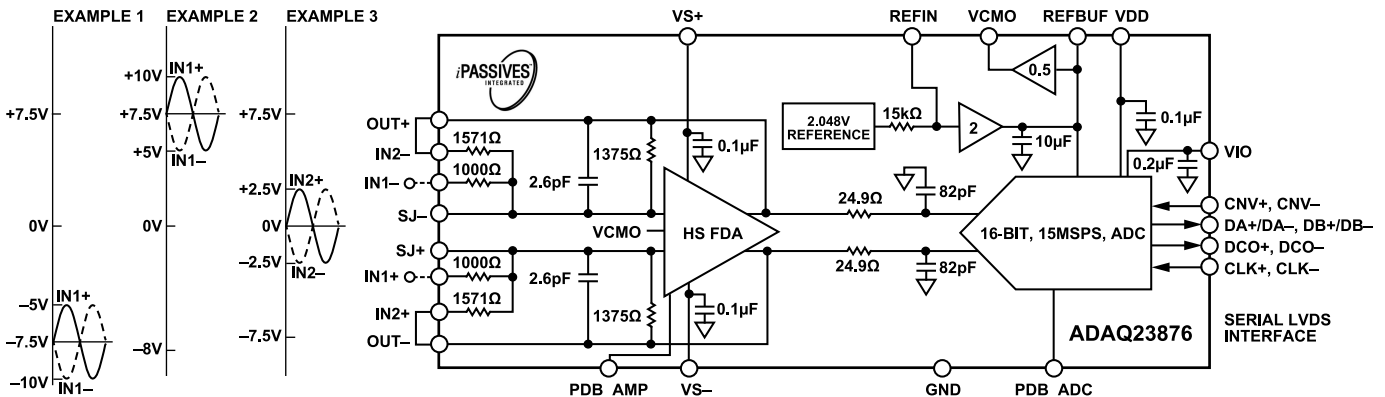


Figure 72. ADAQ23876 Differential Input Configuration with Gain = 0.73,  $\pm 5$  V Input Range

APPLICATIONS INFORMATION

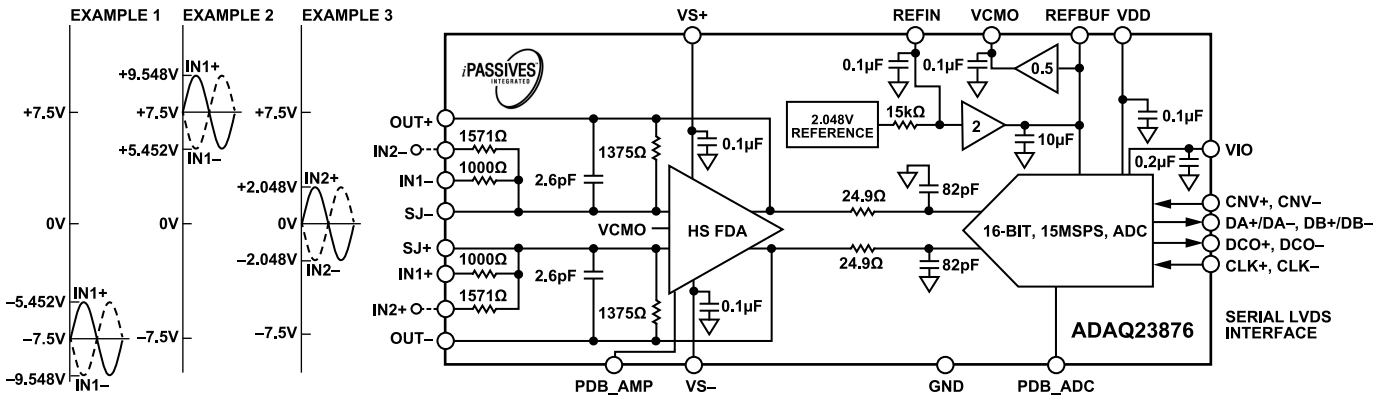


Figure 73. ADAQ23876 Differential Input Configuration with Gain = 0.87, ±4.096 V Input Range

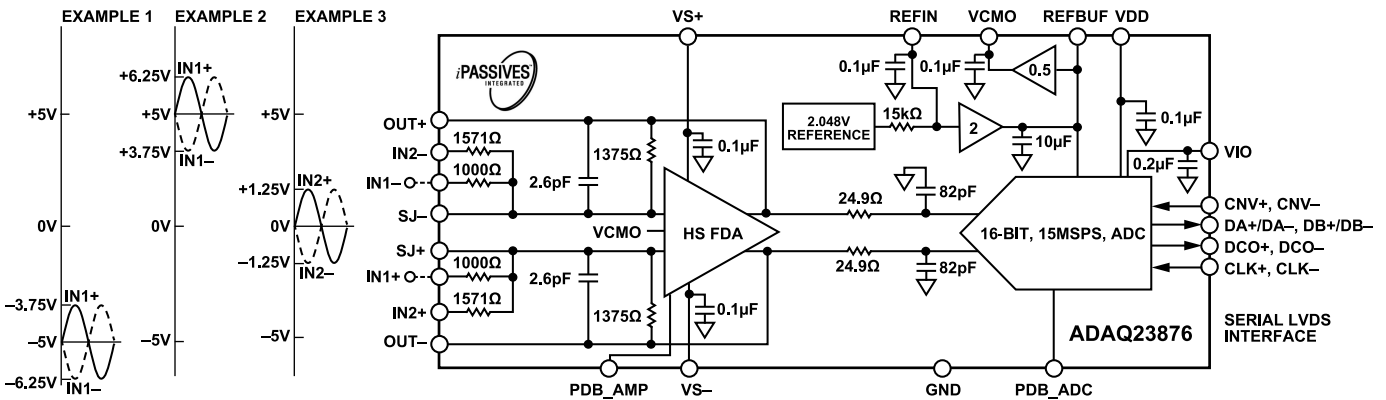


Figure 74. ADAQ23876 Differential Input Configuration with Gain = 1.38, ±2.5 V Input Range

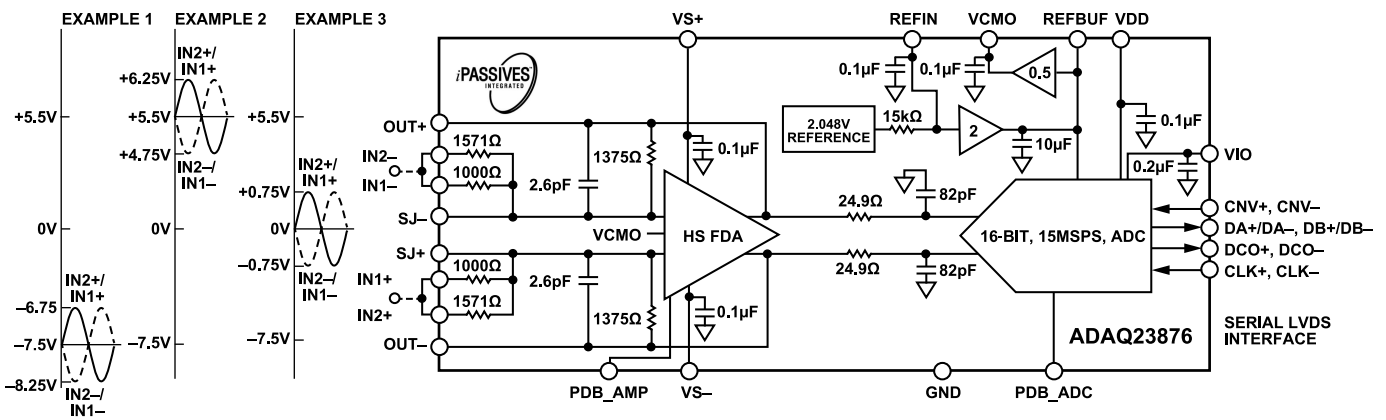


Figure 75. ADAQ23876 Differential Input Configuration with Gain = 2.25, ±1.5 V Input Range

APPLICATIONS INFORMATION

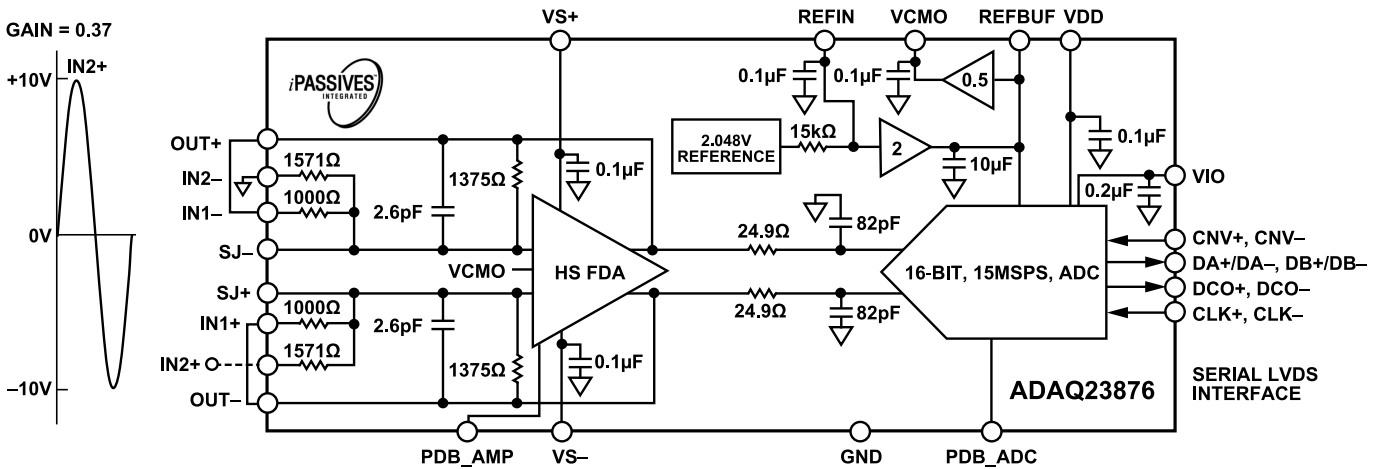


Figure 76. ADAQ23876 Single-Ended Input Configuration with Gain = 0.37

077

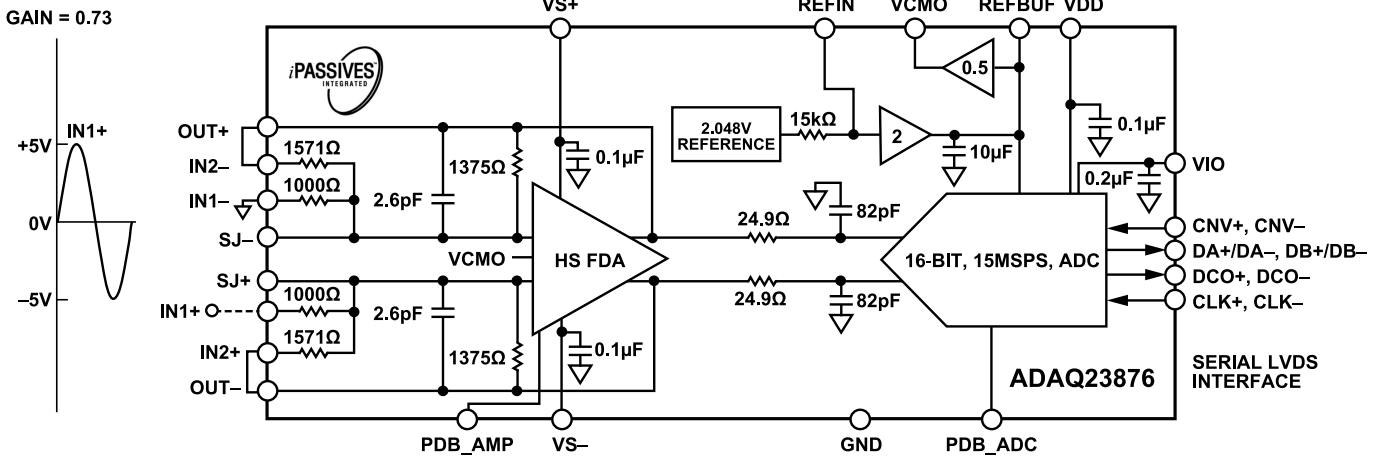


Figure 77. ADAQ23876 Single-Ended Input Configuration with Gain = 0.73

078

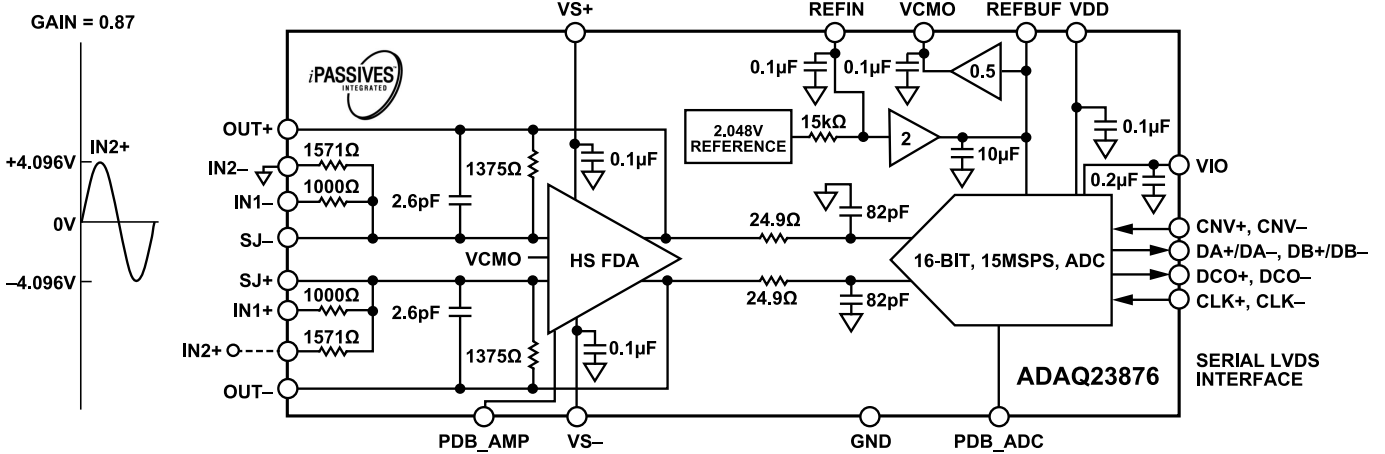


Figure 78. ADAQ23876 Single-Ended Input Configuration with Gain = 0.87

079

APPLICATIONS INFORMATION

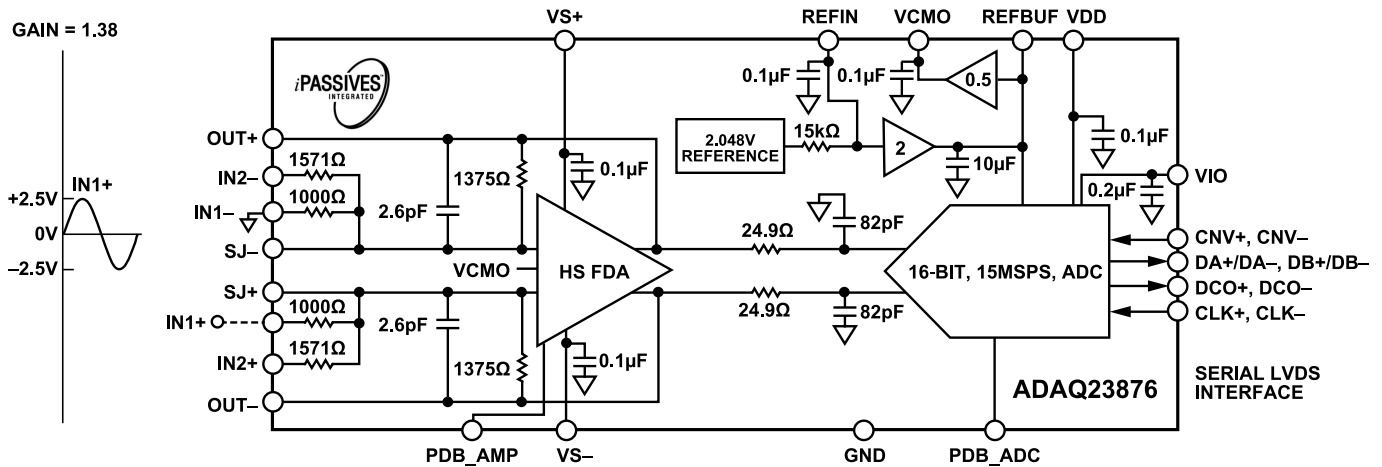


Figure 79. ADAQ23876 Single-Ended Input Configuration with Gain = 1.38

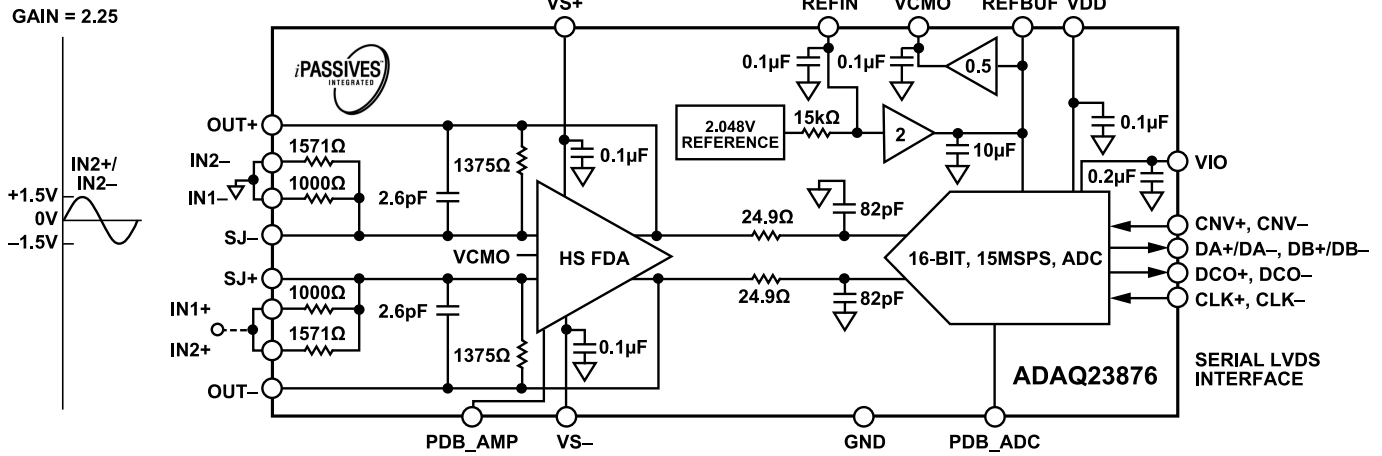


Figure 80. ADAQ23876 Single-Ended Input Configuration with Gain = 2.25

## APPLICATIONS INFORMATION

### VOLTAGE REFERENCE INPUT

The ADAQ23876  $\mu$ Module has an internal low noise, low drift (20 ppm/ $^{\circ}$ C), band gap reference connected to REFIN. An internal reference buffer gains the REFIN voltage by  $2\times$  to 4.096 V at the REFBUF pin. The voltage difference between REFBUF and GND determines the full-scale input range of the ADAQ23876. The common-mode voltage of VCMO and LVDS pins are derived from REFBUF. Therefore, a voltage at REFBUF pin must be stable after the ADAQ23876 is powered on or exits power-down mode before starting a conversion cycle. The reference and reference buffer can also be externally driven if desired. Also housed in the ADAQ23876 is a 10  $\mu$ F decoupling capacitor between REFBUF and GND that is ideally laid out within the device. This decoupling capacitor is a required component of the SAR architecture. Adding a second, smaller capacitor in parallel with the 10  $\mu$ F capacitor may degrade performance and is not recommended.

#### Internal Reference with Internal Reference Buffer

To use the internal reference and internal reference buffer, bypass the REFIN pin to GND with a 0.1  $\mu$ F ceramic capacitor.

#### External Reference with Internal Reference Buffer

If more accuracy and/or lower drift is desired, REFIN can be directly overdriven by an external 2.048 V reference as shown in Figure 81. Analog Devices offers a portfolio of high performance references designed to meet the needs of many applications. With small size, low power, and high accuracy, the LTC6655 is well suited for use with the ADAQ23876 when overdriving the internal reference. The LTC6655 offers 0.025% (maximum) initial accuracy and 2 ppm/ $^{\circ}$ C (maximum) temperature coefficient for high precision applications.

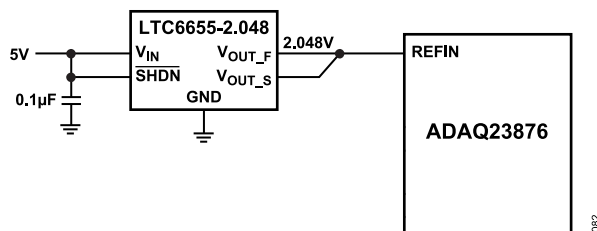


Figure 81. Using the LTC6655 as an External Reference

#### External Reference Buffer

The internal reference buffer can also be overdriven with an external 4.096 V reference at REFBUF as shown in Figure 82. To do so, REFIN must be grounded to disable the reference buffer. The external reference must have a fast transient response and be able to drive the 0.5 mA to 1.6 mA load at the REFBUF pin. The LTC6655 is recommended when overdriving REFBUF.

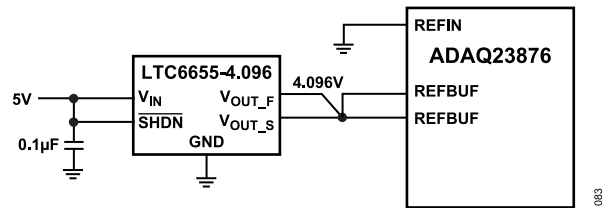


Figure 82. Overdriving REFBUF Using the LTC6655

### COMMON-MODE OUTPUT

The VCMO pin is an output that provides one half the voltage present on the REFBUF pin. This voltage is used to set the common mode of a differential amplifier driving the analog inputs. If VCMO is not used, it can be left floating, but the parasitic capacitance on the pin must be under 10 pF.

### POWER SUPPLY

The ADAQ23876 uses four power supplies: an internal ADC core supply (VDD), a digital input/output interface supply (VIO), a fully differential ADC driver positive supply (VS+), and a negative supply (VS-). Figure 58 shows the typical total power dissipation including individual consumption for each of the VS+, VDD, and VIO supplies. It is recommended to bypass each of the supply pins (VDD, VIO, VS+, and VS-) with a 2.2  $\mu$ F (0402, X5R) ceramic decoupling capacitor connected to GND. See the Board Layout section for the layout guidelines.

#### Power Supply Sequencing

The ADAQ23876 does not have any specific power supply sequencing requirements. The internal ADC core of ADAQ23876 has a power-on-reset (POR) circuit that resets the ADAQ23876 at initial power-up or whenever VDD drops well below the minimum values. After the supply voltage re-enters the nominal supply voltage range, the POR reinitializes the ADAQ23876. After the ADAQ23876 is powered on or exits power-down mode, conversion data is invalid for the first two conversion cycles. The subsequent conversion results are accurate as long as the time between conversions meets the  $t_{CYC}$  specification.

#### Power-Down Mode

The power-down mode of fully differential ADC driver is asserted by applying a low logic level (GND) to the PDB\_AMP pin to minimize the quiescent current consumed when the ADAQ23876 is not being used. When the PDB\_AMP pin is connected to GND, the fully differential ADC driver output is high impedance. When PDB\_ADC is low logic level, an internal ADC core enters power-down mode, and all circuitry (including the LVDS interface) is shut down. When PDB\_AMP and PDB\_ADC are connected to a high logic level, the ADAQ23876 operates normally. The logic levels for both the PDB\_AMP and PDB\_ADC pins are determined by VS+ and VIO, respectively.

## APPLICATIONS INFORMATION

In power-down state, all internal ADC functions, including the reference and LVDS outputs, are turned off and subsequent conversion requests are ignored. This mode can be used if the ADAQ23876 is inactive for a long period of time and the user wants to minimize power dissipation. The amount of time required to recover from power-down mode depends on how REFBUF is configured. When using the internal reference buffer, the internal ADC core stabilizes after 20 ms. If REFBUF is externally driven, the recovery time can be significantly less.

## DIGITAL INTERFACE

The ADAQ23876 conversion is controlled by the CNV+ and CNV- inputs, which can be driven directly with an LVDS signal. Alternatively, the CNV+ pin can be driven with a 0 V to 2.5 V CMOS signal when CNV- is connected to GND. A rising edge on CNV+ samples the analog inputs and initiates a conversion. The pulse width of CNV+ must meet the  $t_{CNVH}$  and  $t_{CNVL}$  specifications in the timing table (see [Table 2](#)).

After the ADAQ23876 is powered on or exits power-down mode, conversion data is invalid for the first two conversion cycles. The subsequent conversion results are accurate as long as the time between conversions meets the  $t_{CYC}$  specification. If the analog input signal has not completely settled when it is sampled, the ADAQ23876 noise performance is affected by jitter on the rising edge of CNV+. In this case, drive the rising edge of CNV+ with a clean, low jitter signal. Note that the ADAQ23876 is less sensitive to jitter on the falling edge of CNV+. In applications that are insensitive to jitter, CNV can be driven directly from a field programmable gate array (FPGA).

The ADAQ23876 has an internal clock that is trimmed to achieve a maximum conversion time of 63 ns. With a typical acquisition time of 27.7 ns, throughput performance of 15 MSPS is achieved.

The ADAQ23876 has a serial LVDS digital interface that is easy to connect to an FPGA. Three LVDS pairs are required: CLK±, DCO±, and DA±. A fourth LVDS pair, DB±, is optional (see [Figure 83](#)). Route the LVDS signals on the PCB as 100  $\Omega$  differential transmission lines and terminated at the receiver with 100  $\Omega$  resistors. The optional LVDS output, DB±, is enabled, and data is output two bits at a time on DA± and DB±. Enabling the DB± output increases the supply current from VIO by about 3.6 mA. In two-lane mode, four clock pulses are required for CLK± (see [Figure 87](#)).

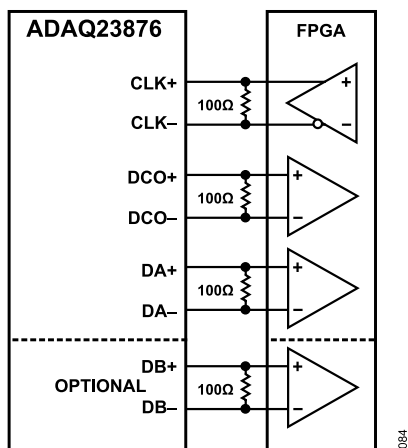


Figure 83. Digital Output Interface to an FPGA

## ONE-LANE OUTPUT MODE

A conversion is started by the rising edge of CNV+. When the conversion is complete, the most significant data bit is output on DA±. Data is then ready to be shifted out by applying a burst of eight clock pulses to the CLK± input. The data on DA± is updated by every edge of CLK±. An echoed version of CLK± is output on DCO±. The edges of DA± and DCO± are aligned. Therefore, DCO± can be used to latch DA± in the FPGA. The timing of a single conversion is shown in [Figure 84](#) and [Figure 85](#). Data must be clocked out after the current conversion is complete, and before the next conversion finishes. The valid time window for clocking out data is shown in [Figure 86](#). Note that it is allowed to be still clocking out data when the next conversion begins.

## TWO-LANE OUTPUT MODE

At high sample rates, the required LVDS interface data rate can reach >400 Mbps. Most FPGAs can support this rate, but if a lower data rate is desired, the two-lane output mode can be used. When the TWOLANES input pin is connected high (VIO), the ADAQ23876 outputs two bits at a time on DA-/DA+ and DB-/DB+, as shown in [Figure 87](#).

DIGITAL INTERFACE

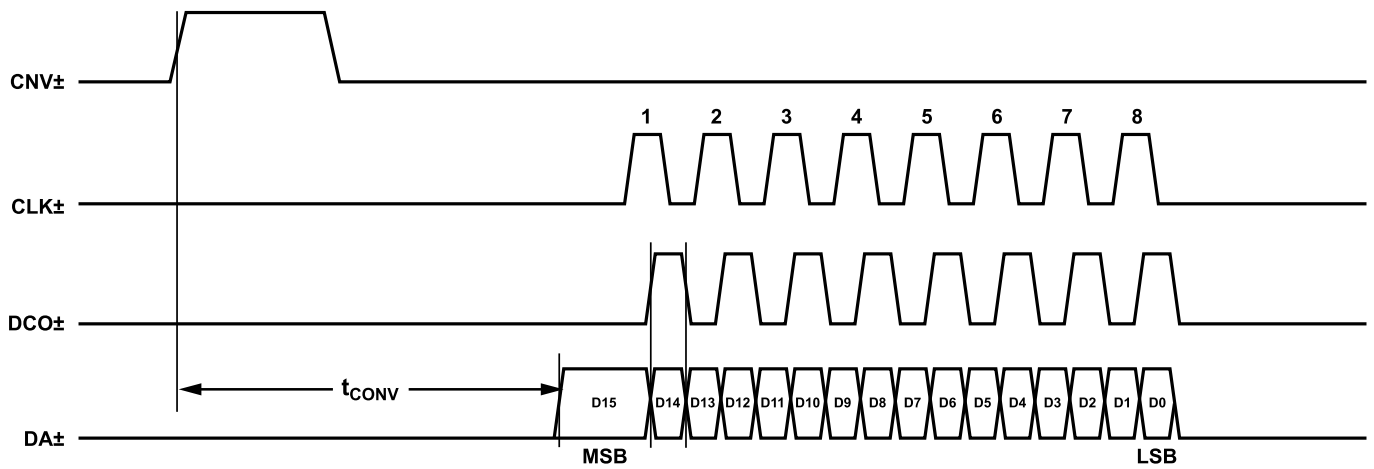


Figure 84. Timing Diagram for a Single Conversion in One-Lane Mode

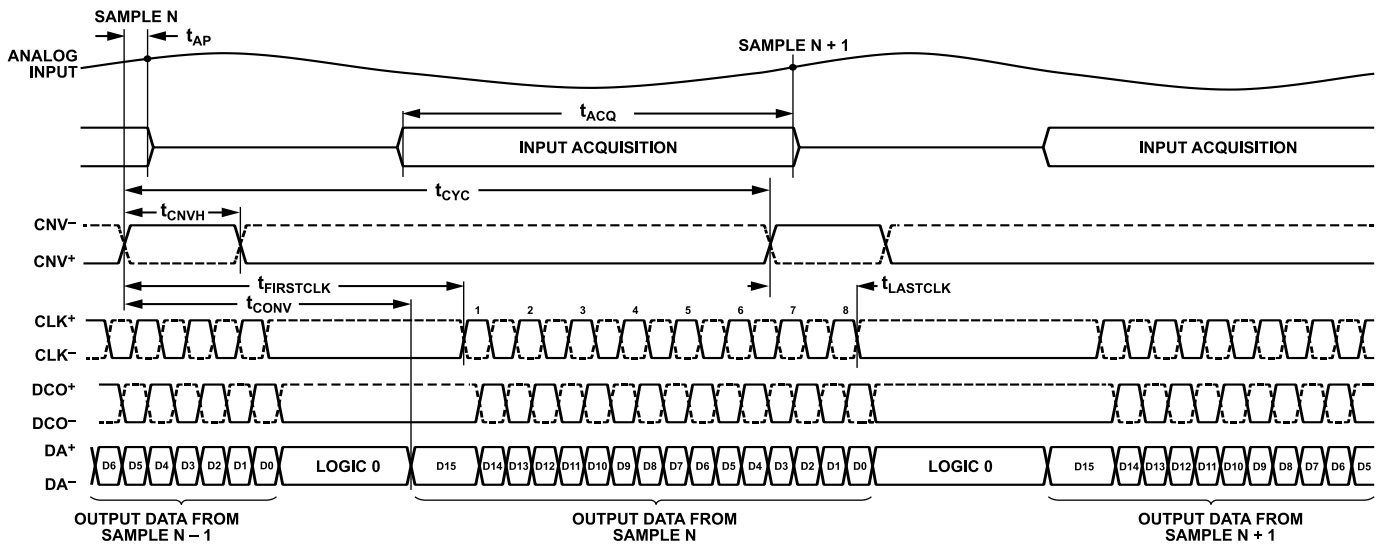


Figure 85. Timing Diagram for Multiple Conversions in One-Lane Output Mode

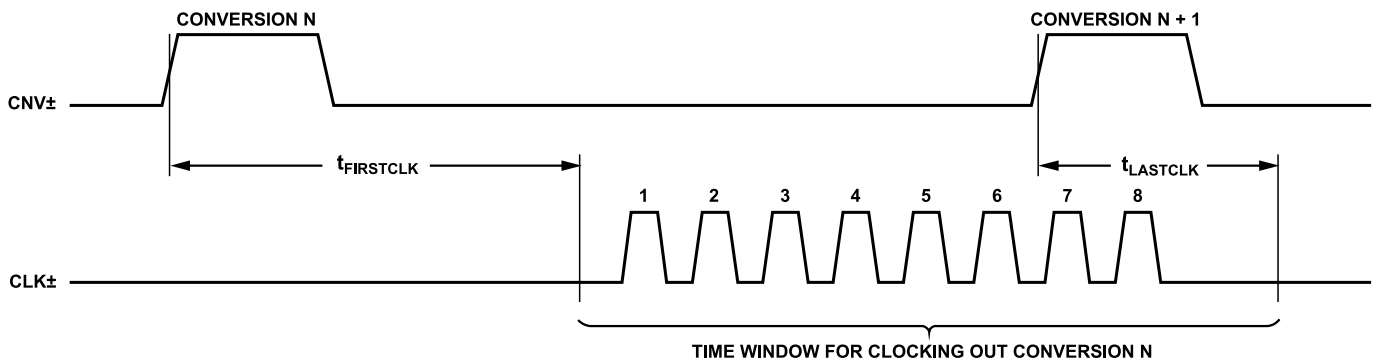


Figure 86. Valid Time Window for Clocking Out Data

DIGITAL INTERFACE

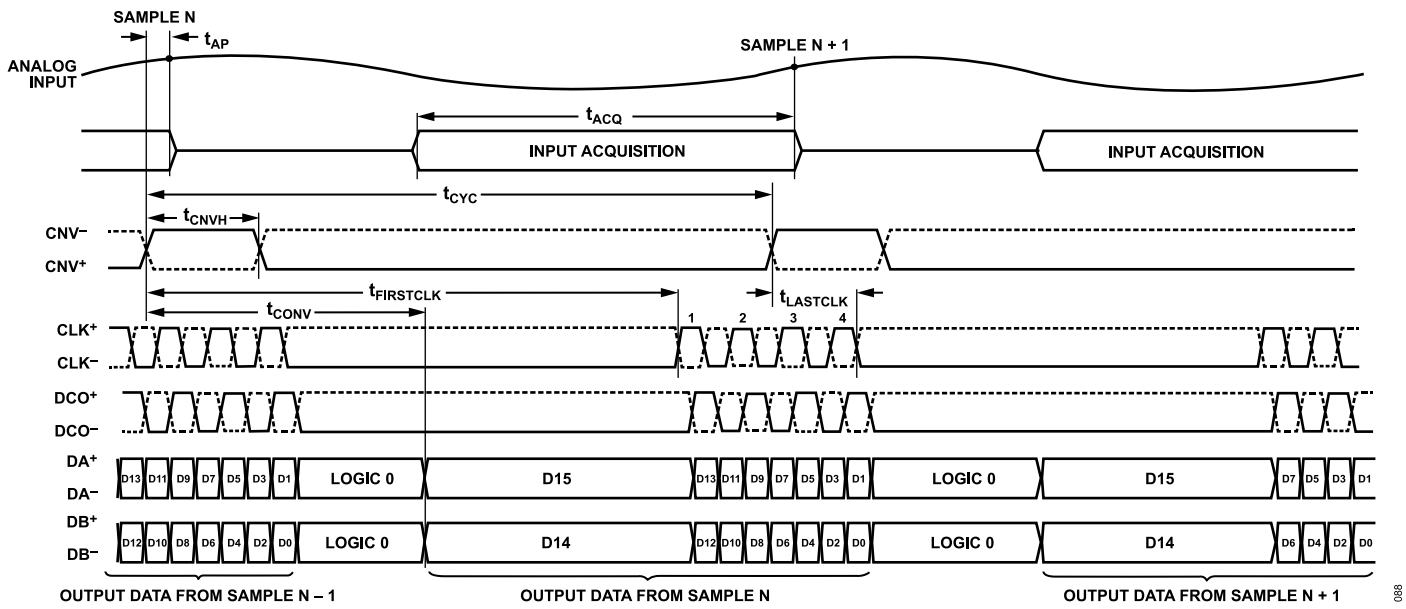


Figure 87. Two-Lane Output Mode

## DIGITAL INTERFACE

### OUTPUT TEST PATTERNS

The test pattern is enabled when the TESTPAT pin is brought high (VIO) to allow in-circuit testing of the digital interface of the ADAQ23876 and forces the LVDS data outputs to be a test pattern. The ADAQ23876 digital data outputs known values as a test pattern as follows:

- ▶ One-lane mode: 1010 0000 0111 1111
- ▶ Two-lane mode: 1100 1100 0011 1111

When the TESTPAT pin is connected low (GND), the ADAQ23876 digital data outputs the conversion results.

## BOARD LAYOUT

The PCB layout is critical for preserving signal integrity and achieving the expected performance from the ADAQ23876. A multilayer board with an internal, clean ground plane in the first layer beneath the ADAQ23876 is recommended. Care must be taken with the placement of individual components and routing of various signals on the board. It is highly recommended to route input and output signals symmetrically. Solder the ground pins of the ADAQ23876 directly to the ground plane of the PCB using multiple vias. Remove the ground and power planes beneath the input and output pins of ADAQ23876 to avoid undesired parasitic capacitance. Any undesired parasitic capacitance could impact the distortion and linearity performance of the ADAQ23876.

The pinout of the ADAQ23876 eases the layout and allowing its analog signals on the left side and its digital signals on the right side. The sensitive analog and digital sections must be separated on the PCB while keeping the power supply circuitry away from the analog signal path. Fast switching signals, such as  $CNV_{\pm}$  or  $CLK_{\pm}$ , and digital outputs  $DA_{\pm}$  and  $DB_{\pm}$  must not run near or cross over analog signal paths to prevent noise coupling to the ADAQ23876.

Good quality ceramic bypass capacitors of at least  $2.2\ \mu\text{F}$  (0402, X5R) must be placed between each of supply pins ( $VDD$ ,  $VIO$ ,  $VS+$ , and  $VS-$ ) of the ADAQ23876 and GND to minimize electromagnetic interference (EMI) susceptibility and to reduce the effect of glitches on the power supply lines. All the other required bypass capacitors are laid out within the ADAQ23876, saving extra board space and cost.

Figure 88 shows the FFT sampling of the ADAQ23876 at 15 MSPS with the inputs shorted when the external decoupling capacitors on the  $REFIN$ ,  $VDD$ , and  $VIO$  pins near the  $\mu\text{Module}$  are removed and how well  $\mu\text{Module}$  rejects any supply noise and reduces sensitivity to perturbations. This performance impact was verified on the [EVAL-ADAQ23876FMCZ](#) and no spurs are present in the noise floor, regardless of whether these external decoupling capacitors are used or removed. The recommended board layout is described in the EVAL-ADAQ23876FMCZ user guide.

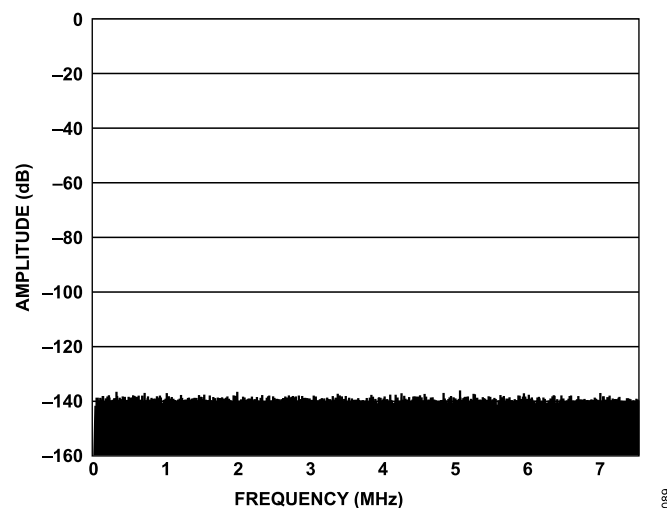


Figure 88. FFT with Shorted Inputs

## MECHANICAL STRESS SHIFT

The mechanical stress of mounting a device to a board may cause subtle changes to the SNR and internal voltage reference. The best soldering method is to use IR reflow or convection soldering with a controlled temperature profile. Hand soldering with a heat gun or a soldering iron is not recommended.

OUTLINE DIMENSIONS

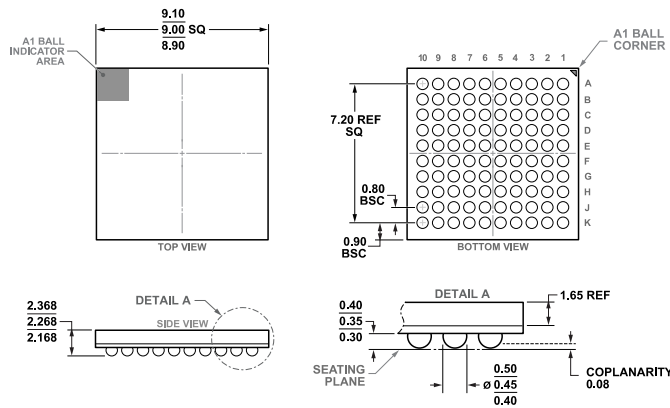


Figure 89. 100-Ball Chip Scale Package Ball Grid Array [CSP\_BGA] (BC-100-7)  
Dimensions shown in millimeters

ORDERING GUIDE

Model <sup>1</sup>	Temperature Range	Package Description	Packing Quantity	Package Option
ADAQ23876BBCZ	-40°C to +85°C	100-Ball CSP-BGA (9mm x 9mm x 2.268mm)	Tray, 260	BC-100-7

<sup>1</sup> Z = RoHS Compliant Part.

Updated: August 09, 2023

EVALUATION BOARDS

Model <sup>1</sup>	Description
EVAL-ADAQ23876FMCZ	Evaluation Board

<sup>1</sup> Z = RoHS Compliant Part

Legal Terms and Conditions

Information furnished by Analog Devices is believed to be accurate and reliable "as is". However, no responsibility is assumed by Analog Devices for its use, nor for any infringements of patents or other rights of third parties that may result from its use. Specifications subject to change without notice. No license is granted by implication or otherwise under any patent or patent rights of Analog Devices. Trademarks and registered trademarks are the property of their respective owners. All Analog Devices products contained herein are subject to release and availability.